TALLINN UNIVERSITY OF TECHNOLOGY
SCHOOL OF ENGINEERING
Department of materials and environmental technology

DEVELOPMENT OF NiO_X THIN FILMS FOR SEMI-TRANSPARENT SOLAR CELLS

NiO_x õhukesekileliste kihtide väljatöötamine poolläbipaistvate päikeseelementide jaoks

MASTER THESIS

Student: Ajibola Abdulahi Bakare

Student code: 214141KAYM

Supervisors: Dr. Nicolae Spalatu
Dr. Atanas Katerski

Tallinn 2023

(*On the reverse side of title page*)

AUTHOR'S DECLARATION

Hereby I declare, that I have written this thesis independently.
No academic degree has been applied for based on this material. All works, major viewpoints and data of the other authors used in this thesis have been referenced.

"24th" May 2023

Author: Ajibola Abdulahi Bakare
/signature /

Thesis is in accordance with terms and requirements

"24th" May 2023

Supervisor: Dr. Nicolae Spalatu
/signature/

Accepted for defence

"24th" May 2023

Chairman of theses defence commission: .....
/name and signature/

Non-exclusive licence for reproduction and publication of a graduation thesis[1]

I Ajibola Abdulahi Bakare,

1. grant Tallinn University of Technology free licence (non-exclusive licence) for my thesis "Development of NiO_x thin films for semi-transparent solar cells",

supervised by Dr. Nicolae Spalatu and Dr. Atanas Katerski,

1.1 to be reproduced for the purposes of preservation and electronic publication of the graduation thesis, incl. to be entered in the digital collection of the library of Tallinn University of Technology until expiry of the term of copyright;

1.2 to be published via the web of Tallinn University of Technology, incl. to be entered in the digital collection of the library of Tallinn University of Technology until expiry of the term of copyright.

2. I am aware that the author also retains the rights specified in clause 1 of the non-exclusive licence.

3. I confirm that granting the non-exclusive licence does not infringe other persons' intellectual property rights, the rights arising from the Personal Data Protection Act or rights arising from other legislation.

24.05.2023

Faculty of Chemical and Materials Technology

---

[1] *The non-exclusive licence is not valid during the validity of access restriction indicated in the student's application for restriction on access to the graduation thesis that has been signed by the school's dean, except in case of the university's right to reproduce the thesis for preservation purposes only. If a graduation thesis is based on the joint creative activity of two or more persons and the co-author(s) has/have not granted, by the set deadline, the student defending his/her graduation thesis consent to reproduce and publish the graduation thesis in compliance with clauses 1.1 and 1.2 of the non-exclusive licence, the non-exclusive license shall not be valid for the period.*

THESIS TASK

Student: Ajibola Abdulahi Bakare, 214141KAYM
Study programme, main speciality: Materials and Processes for Sustainable Energetics
Materials for sustainable energetics
Supervisor(s): Research Scientist, Dr. Nicolae Spalatu, +3726203366
Research Scientist, Dr. Atanas Katerski, +3726203369

Thesis topic:
(in English) DEVELOPMENT Of NiO_x THIN FILMS FOR SEMI-TRANSPARENT SOLAR CELLS
(in Estonian) NiO_x õhukesekileliste kihtide väljatöötamine poolläbipaistvate päikeseelementide jaoks

Thesis main objectives:

1. To acquire knowledge of ultrasonic spray pyrolysis technique for the deposition of metal oxide thin films.
2. To obtain knowledge on material (thin films) characterization techniques.
3. To develop NiO_x thin films by ultrasonic spray pyrolysis (USP) technique and investigate the influence of USP deposition conditions, including the deposition temperature.
4. To implement the use of the fuel (acetylacetone) in the precursor solution for the ultrasonic spray pyrolysis process.
5. To represent and discuss the impact of post deposition treatment on the structural and optoelectronic properties of NiO_x films.
6. To discuss the mechanism of physicochemical processes responsible for changes in the properties of the films depending on the deposition variables.

Thesis tasks and time schedule:

No	Task description	Deadline
1.	USP-deposition of first sample set ($NiNO_3$:AcAcH 5:1) at different temperatures, material characterization of the samples (UV-VIS, XRD, van der Pauw)	
2.	USP-deposition of second sample set ($NiNO_3$:AcAcH 5:2), material characterization of the samples (UV-VIS, XRD, SEM, van der Pauw)	
3.	USP-deposition of third sample set ($NiNO_3$:AcAcH 5:3), material characterization of the samples (UV-VIS, XRD, van der Pauw)	

4	Analysis of derived data and thesis writing	

Language: English **Deadline for submission of thesis:** "24th" May 2023

Student: Ajibola Abdulahi Bakare ..... "24th" May 2023
/signature/

Supervisor: Dr. Nicolae Spalatu ..... "24th" May 2023
/signature/

Co-Supervisor: Dr. Atanas Katerski ..... "24th" May 2023
/signature/

Head of study programme: Prof. Sergei Bereznev ..... "24th ", May 2023
/signature/

CONTENTS

PREFACE

The idea of the thesis was proposed by Dr. Nicolae Spalatu and Dr. Abayomi Oluwabi, with the work conducted in the Laboratory of Thin Film Chemical Technologies. My heartfelt appreciation goes to my supervisors Dr. Nicolae Spalatu and Dr. Atanas Katerski for their technical support, wealth of experience, discussions and being available to provide solutions to the challenges faced during this research. A notable mention to Dr. Abayomi Oluwabi for supporting with the design of the thesis tasks. A special appreciation to Prof. Sergei Bereznev for making mine and my colleagues stay in the program an experience to remember. I would like to express my gratitude to Prof. Malle Krunks, Prof. Ilona Oja Acik for making the lab a place to be. I would also like to extend my gratitude to Mykhailo Koltsov for being an accessible and willing help in this work. I am indeed grateful to Dr. Olga Volobujeva for helping with SEM imaging. This study was financially supported by Estonian Research Council project PRG627 "Antimony chalcogenide thin films for next-generation semi-transparent solar cells applicable in electricity producing windows". Estonian Research Council project PSG689 "Bismuth Chalcogenide Thin-Film Disruptive Green Solar Technology for Next-Generation Photovoltaics." Estonian Centre of Excellence project TK141 (TAR16016EK) "Advanced materials and high-technology devices for energy recuperation systems." The European Union's H2020 Programme under the ERA Chair project 5GSOLAR grant agreement No. 952509.

Short summary

The focus of this research was to understand the USP techniques and their application for the deposition of nickel oxide film for hole transport layer application and the effect of deposition temperature and the effect of the fuel (acetylacetone) on the film properties. This led to gaining more insight into USP, nickel oxide film as hole transport material, and some characterization techniques. Herein, NiO_x films were deposited on borosilicate glass varying the temperature between 200 to 400 ^oC to determine the optimal temperature. It was concluded the optimal temperature was 400 ^oC. The mole ratio of acetylacetone; a fuel component of the precursor mix was varied between 1 to 3 molar ratio and effect on the NiO_x film deposition process. Highest crystallite size and transparency of 32.4 nm and 70% respectively was attained for the $NiNO_3$:AcAcH 5:3 thin film. Band gap of the films decreased from 3.61 to 3.53 eV as the molar ratio of the acetylacetone fuel in the precursor mix increased from 5:1 to 5:3.

Keywords: NiO_x; ultrasonic spray pyrolysis; nickel nitrate; acetylacetone; master thesis

List of abbreviations and symbols

□ absorption coefficient

AcAcH acetylacetone

CBD chemical bath deposition

CSP chemical spray pyrolysis

CVD chemical vapor deposition

d thickness

E_g band gap energy

ESP Electrostatic spray pyrolysis

EtOH ethanol

HTL Hole transport layer

ITO Indium tin oxide

JCPDS Joint Committee on Powder Diffraction Standards

LED- light emitting diode

NiOx- Nickel oxide

PSP- Pneumatic spray pyrolysis

SPT- Spray pyrolysis technique

T- transmission

USP- ultrasonic spray pyrolysis

UV-Vis- ultraviolet-visible

XRD- x-ray diffraction

1. INTRODUCTION

The demand for electricity or power has been on the increase with the growing world population. Around a quarter of the human population has been reported to be with little to no access to power over the past number of years [1]. This increasing demand for energy cannot be fully catered for by fossil fuels alone alongside their environmental concern, hence the need for renewable energy as a possible solution to the challenge.

Renewable energy sources have been an increasing area of research in recent years due to their importance in addressing the energy deficits that sets in in the light of the reduction in fossil fuel reserves and increasing global warming. Sources of energy like wind, hydro, geothermal, biomass, tidal, and solar have been explored to increase the supply of energy due to their renewability and potential [2].

PV technology is an appealing option and prospect due to its abundance, availability, and non-emission of carbon dioxide. This is evident in the pace of growth of solar PV system installations around the world. This growth has been driven by research into making solar cells more flexible, portable, and increased efficiency [3].

Globally, the photovoltaic capacity was around 591 GW, with an average yearly compound growth rate of more than 35%. This growth rate can be linked in large part to solar technology development, complementary energy policy, and the sharp reduction in cost. The growth of PV technology globally will be on the rise as more of the world's energy portfolio is shifted towards filling by renewables, taking into consideration its increasing cost-friendliness [4].

Crystalline silicon cells, a device that uses light energy to produce electricity are considered an expensive device to produce, with the assembling of its modules seemingly a complex task, thereby making the emergence of thin film technology an interesting alternative. These thin films are relatively cheaper compared to silicon cells and can be produced by deposition of a semi-conductive material layer on a substrate (e.g. glass, polymer) [5].

Thin films like TiO_2, NiO_x, and CdS have been deposited for different applications that range from gas sensors, and photocatalysts to photovoltaics [6], [7]. NiO_x is a semiconductor with a wide bandgap usually in the range of 3.5 eV to 4.3 eV [8] that has been studied for its potential applications ranging from thermoelectric devices [9], antireflection coatings, optical sensor technology [10], absorber layer and hole transport layer [11]. The chemical stability and high transmittance it possesses contribute to making it an attractive metal oxide.

This film has been reported to be deposited using a range of techniques cutting across physical and chemical deposition methods. Techniques like electron beam evaporation [11], spin coating [12], sol-gel [13][14] and spray pyrolysis [15]–[18] has been

explored in the deposition of NiO_x thin film. Ultrasonic spray pyrolysis technique as a technique has gained more attention due to its low economic outlay, ease of scale up to industrial scale, application without vacuum, and its simplicity.

Varieties of precursors have been used for the deposition with varied results, nickel acetate, nickel nitrate, nickel chloride, and nickel acetylacetonate being the prominent ones [13][18][19].

The present investigation is geared towards optimizing the deposition temperature of NiO_x films using ultrasonic spray pyrolysis technique, deposition of NiO_x thin film on glass substrate while investigating the impact of the fuel component ratio (acetyacetone of the precursor material on the quality of films deposited. The effect of post-deposition heat treatment on the film's properties is of similar interest. The deposited films were characterized using XRD, UV-Vis spectroscopy, van der Pauw measurement, and scanning electron microscopy.

2. BACKGROUND AND LITERATURE REVIEW

2.1 Thin film solar cell

Thin film can be described to be a material formed or fabricated by the nucleation and growth of individually reacting chemical species on a substrate serving as a base or support to build on. This film regarded as thin, has a thickness ranging from a few nanometres to a few tens of microns. Such film property, be it chemical, mechanical, or structural is largely dependent on the deposition parameters and often thickness-dependent [20][21].

Thin film solar cell is a device made up of different layers that are in thin film form. These layers have their individual properties which directly or indirectly influence the final performance of the final device. This solar cell absorbs light and transforms the photons of light into electric current, exhibiting what is referred to as the photovoltaic effect [21].

2.1.1 Structure of thin film solar cell

A thin film solar cell has its layers arranged in two possible forms: the superstrate and substrate configurations as shown in Fig 1. Superstrate configuration thin films are deposited in a top-down approach, with the first layer deposited being the point of entry for light; the transparent conducting oxide layer, through the other layers required for the solar cell, ending with the deposition of the back contact. This form of thin film solar cell configuration requires a highly transparent substrate to ease the passage of light to the absorber.

Substrate configuration has the layers deposited in a bottom-to-top style, starting with the back contact like Mo/Au up to the transparent conducting oxide layer at the top of the solar cell which as stated earlier is the point of entry for light energy. The use of transparent substrates is not a necessity in this configuration, hence non-transparent materials can be used as substrates [22].

The structure of thin film solar cells consists of the substrate, transparent conducting oxide (TCO), hole transport layer (HTL), absorber layer, electron transport layer (ETL), and back contact.

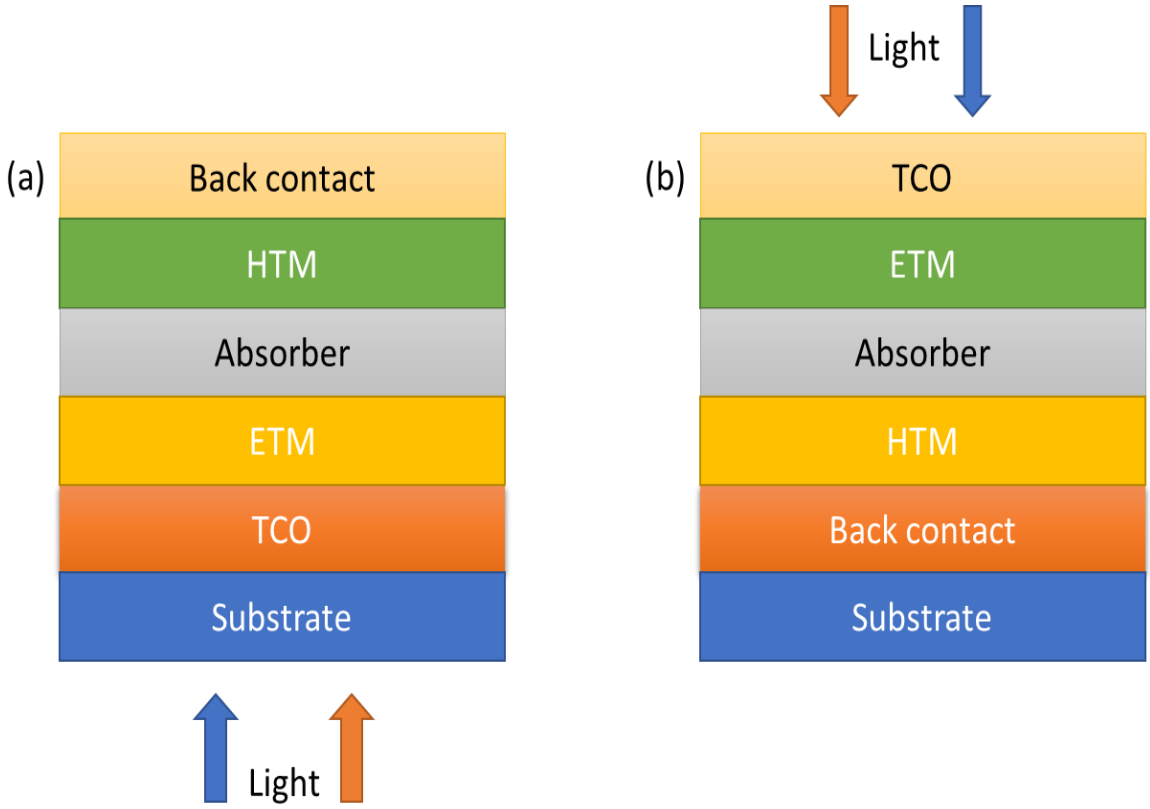

Figure 1. Thin Film Solar cell configurations (a) Superstrate (b) Substrate [42]

The electron transport layer ETL is a layer that should have a wide bandgap to allow the passage of light to the absorber. This layer is usually an n-type material with the ability to form a heterojunction with a p-type absorber. Examples of widely used ETL or buffer layers in thin film applications are cadmium sulphide, titanium dioxide, and zinc oxide. Hole transport layer HTL is a layer meant for extracting and increasing the transportation of holes, preventing quenching, and is made towards preventing the drift of electrons towards the back contact. Materials meant for HTL application need to possess high work function and should be transparent. HTLs range from inorganic semiconductors to polymers, with copper iodide (CuI), copper thiocyanate (CuSCN), and nickel oxide (NiO_x) being some of the inorganics used for this purpose [12][23].

A substrate must be not an active component of the solar device, inert during the fabrication of the device. The choice of substrate is dictated by the application and orientation of the cell whether it is a superstrate or substrate configuration as earlier indicated where superstrate configuration requires a transparent substrate and vice versa. Depending on the purpose, substrates might range from polymer to glass to stainless steel [21]. In our case we choose borosilicate glass, because we wanted to exclude the sodium diffusion during the depositon and thermal treatment of the samples.

Transparent conducting oxide TCO is typically made of n-type semiconductors with strong transparency in the visible region and electrical conductivity. This layer's conductivity is closely related to carrier mobility and concentration. Some of the most often used TCOs are Tin oxide (SnO_2), Fluorine doped tin oxide (FTO), and indium tin oxide (ITO) [21][22].
In most cases, the absorber layer is a p-type semiconductor. It has a lower band gap typically 1-2 eV and a high absorption coefficient > 10^4/cm in the visible and near-infrared region. The absorber layer generates photocarriers, which are then swept away by the depletion area. a-Si, CdTe, CIGS, chalcogenides, and other organic semiconductors are the most well-known absorber layer materials for thin film solar cell applications [21].

Back contacts, examples of which are gold (Au), molybdenum (Mo), silver (Ag), and copper (Cu) are used in extracting the charge in a solar cell to the external load. This contact needs to be a good conductor and be able to form an ohmic contact with the absorber layer. To reach this, the electrode need to have a high work function (>4.7 eV), because usually absorber layer have high work function as well [21].
NiO_x thin films are one of the most important metal oxides in HTL for developing third and fourth-generation solar cells due to their low toxicity, transparency in visible light range (wide band gap, about 3.6 eV [25]), p-type conductivity, and high stability compared to organic and other popular metal oxides like cuprous oxide (Cu_2O), and tin monoxide (SnO) who are metastable under the same condition, with potential formation of cupric oxide (CuO) and n-type tin (IV) oxide (SnO_2) respectively as phase impurities [24][25]. NiO_x is a relatively abundant material in earth's core and has great potential for use in different devices connecting with sustainable energetics.

2.2 Nickel Oxide

Nickel oxide is an odourless green powder or green-black cubic crystal. It has NiO_x as both empirical and molecular formula, with a molecular weight of 74.69 g. NiO_x crystallizes in a rock-salt crystal structure (NaCl) bunsenite with Ni^{2+} with a valency of 2+ in octahedral coordination with O^{2-} [26]. The crystal structure of NiO_x is shown in Fig 2.

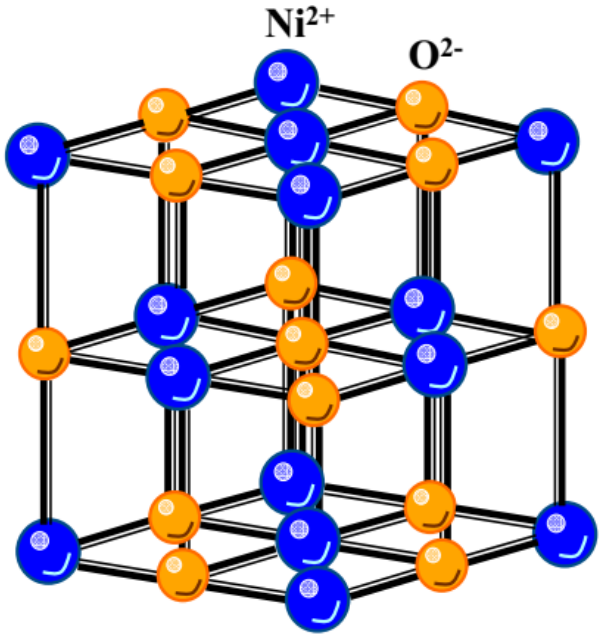

Figure 2. Crystal structure of NiO_x bunsenite [26]

At room temperature, pure stoichiometric nickel oxide is an insulator with electrical conductivity below 10^{-11} Scm^{-1}. The presence of NiO_2H and Ni_2O_3 always indicates the abundance of oxygen in reality. Hence, the need to denote as NiO_x in its non-stoichiometric form. NiO_x is usually a p-type semiconductor as the abundance of oxygen typically brings about holes that form because of Ni vacancies [27].

NiO_x is a semiconductor with a wide bandgap usually in the range of 3.5 eV to 4.3 eV [8] that has been studied for its potential applications ranging from thermoelectric devices [9], antireflection coatings, optical sensor technology [10] to hole transport layer [28]. It has been reported to exhibit p-type conductivity due to nickel vacancies and or interstitial oxygen atoms and it is very stable chemically [8], [14].

Different starting precursors have been reported in the deposition of a nickel oxide thin film with desired properties; nickel acetate, nickel nitrate, nickel chloride [1], nickel acetylacetonate [18].

NiO_x has been reported for its ability to function as a hole transport layer, with some properties being in its support, ranging from its stability, low cost, suitable work function, and energy level matching [12], [28].

Table 2.1 contains some of the reviewed articles showing the precursor, technique, and substrate temperature used in the deposition of some NiO_x thin films.

Table 2.1. Some reviewed NiO_x deposition parameter

Precursor	NiO_x Deposition technique	Substrate Temp. (°C)	Year	Ref.
Nickel chloride hexahydrate	Pneumatic spray pyrolysis (perfume atomizer)	350	2007	[29]
Nickel chloride Nickel nitrate Nickel sulfate Nickel hydroxide	Pneumatic spray pyrolysis (perfume atomizer)	350	2008	[19]
Nickel acetate tetrahydrate	Chemical spray pyrolysis	350 to 450	2010	[8]
Nickel chloride	Simple spray pyrolysis	320, 360, 400	2013	[30]
Nickel acetate	Sol-gel process	550	2014	[31]
Nickel acetate tetrahydrate	Chemical spray pyrolysis	450	2016	[9]
Nickel chloride	Chemical bath deposition Spray pyrolysis	150 to 450	2016	[16]
Nickel nitrate	Pneumatic spray pyrolysis	370 and 420	2016	[15]
Nickel acetate	Sol-gel process	300	2017	[13]
Nickel nitrate	Spray pyrolysis	350 to 390	2019	[17]
Nickel acetate	Sol-gel process	300 to 550	2021	[14]
Nickel acetylacetonate	Ultrasonic spray pyrolysis	450	2023	[18]

2.3 Deposition Methods

A host of deposition techniques have been reported for the deposition of NiO_x thin film; sputtering, vacuum evaporation, and anodic deposition are some of the physical methods employed in previous research about NiO_x deposition [9]. Chemical methods like pneumatic spray pyrolysis [10], [15], chemical spray pyrolysis [8], ultrasonic spray pyrolysis [18] and pulsed spray pyrolysis have also been reported for the synthesis of the films [32].

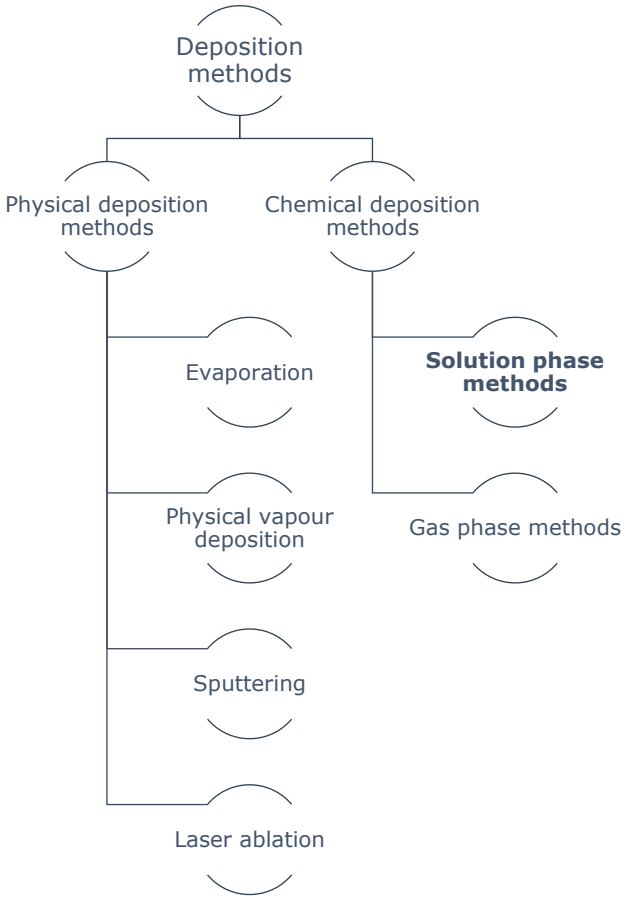

Figure 3. Deposition techniques [20][33]

Various types of deposition techniques are shown in Figure 3 based on the principles driving the deposition [20]. These deposition techniques have been used for the deposition of thin films over the years to varying results, based on the desired properties, and most importantly cost.

Physical methods use a host of vacuum deposition techniques to make coatings and films and can be described as a thin film deposition method that involves the vaporization of solid material in a vacuum onto a substrate as a pure material or doped coating. The films deposited in this manner are usually resistant to abrasion, corrosion and are usually durable. This technique finds application in materials ranging from optics, semiconductors, surgical, and medical implant devices, but the need for vacuum and high cost compared to other thin film techniques is one of the concerns limiting the use of the physical technique of deposition [20].

Chemical deposition method is made up of liquid or solution phase and gas phase deposition techniques. It usually has precursor(s) that are hydrido- or organo-compounds, which on pyrolysis at relatively low-temperature form a thin film and vapor that can be evacuated from the chamber. This technique gives rise to materials that typically maintain bonds in high-stress use, coating of materials with complex

topography, and the ability to use a wide range of substrates material for deposition [20], [33].

2.4 NiO_x thin films by chemical deposition methods

Chemical vapor deposition as a technique involves the transportation of gases, their combination, and chemical reaction on or surrounding a substrate. This reaction of precursor gases with the substrate occurs with the substrate heated, leading to the decomposition of certain parts of the precursor constituents in the gas phase, forming a solid film of the precursor on the substrate [34].

Chemical deposition methods used for the deposition of thin films can be broadly categorized into two based on the phase of the precursor used for the deposition. Chemical vapour is the precursor used for gas phase chemical deposition, while precursor solution is employed in solution phase chemical deposition technique, with the types of chemical deposition shown in Figure 4 [33].

The chemical deposition method can be used on a wide range of substrates, making it one of the advantages of using this technique, alongside the simplicity and cheap cost of processing due to the ability to deposit in little to no vacuum [20]. The gas phase chemical deposition method is subdivided into atomic layer deposition (ALD) and chemical vapor deposition (CVD). The solution phase chemical deposition method is the technique of interest in this research, and it can be further divided into sol-gel, spin coating, spray pyrolysis, and dip coating.

NiO_x thin films have been deposited using a range of chemical deposition methods, from pulsed spray pyrolysis [32], sol-gel [14], [31], chemical spray pyrolysis [8], [9], [35], chemical bath deposition [16].

Some spray pyrolysis methods have been used to deposit NiO_x over the years, pneumatic spray pyrolysis has been reported by Cattin et al, Mahmoud et al, and Reguig et al [10], [19], [29] for the deposition, pulsed spray pyrolysis by Obaida et al [32], ultrasonic spray pyrolysis by [18].

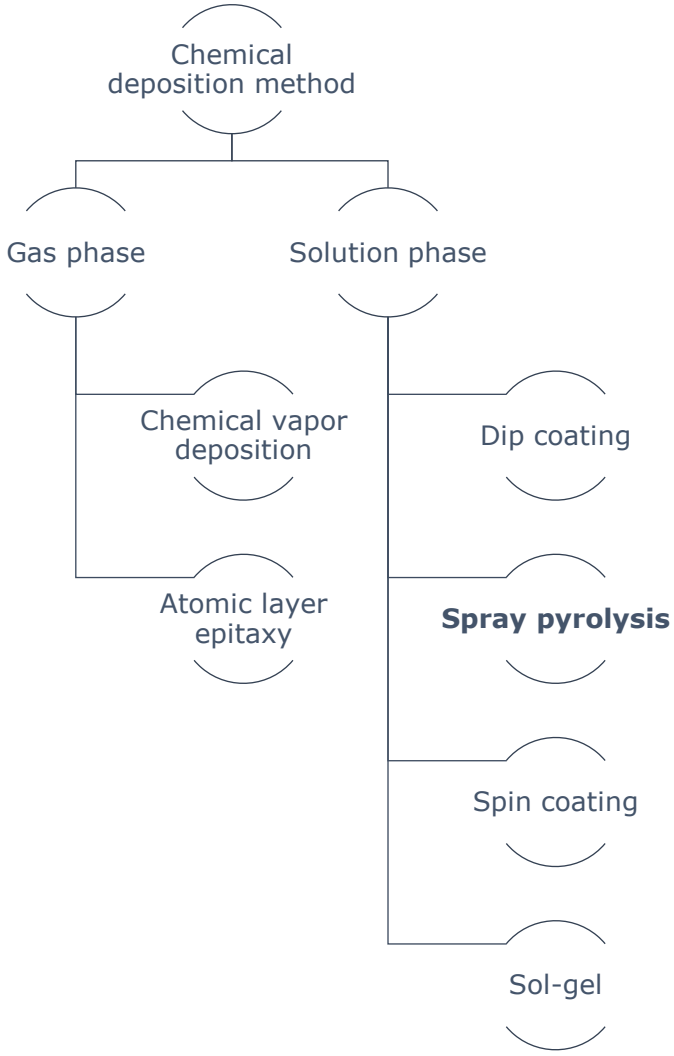

Figure 4. Chemical deposition methods of thin films [33]

2.5 Properties of NiO_x thin films deposited by chemical deposition method

NiO_x thin film has been reported to have been deposited using chemical spray pyrolysis by Romero et al. with the NiO_x film having morphology that is reticular tissue-like, crystallite size of around 10 nm, and band gap reducing from 4.3 eV to 3.65 eV as the film thickness increases [8]. Cattin et al. investigated the use of different precursors in depositing nickel oxide thin films at 350 ^oC, the films were found to be p-type with cubic crystals obtained for the films made from the chlorides and nitrates salts. Annealing of the films in open air was found not to make any significant difference to the films properties but annealing in vacuum yielded better modification compared to the room atmosphere annealing [19]. NiO_x thin film deposited on glass and silicon substrates by

Ismail et al. with spray pyrolysis using hydrated nickel chloride salt solution showed polycrystalline cubic structure with preferred orientation along (111) and (200) plane respectively. The band gaps (3.4 to 3.8 eV) were reported to move inversely to the molarity of the precursor solution, but the electrical resistivity moves directly with the concentration, increasing as concentration increases [30]. Kate et al. investigated the effect of Ts on properties of NiO_x thin films deposited using SPT from hydrated Nickel nitrate salt solution, giving polycrystals of cubic structure with (111) plane preferred orientation and optical band gap ranging between 3.1 eV and 4.0 eV and increasing conductivity as substrate temperature increased [17]. Using hydrated nickel chloride, Gomaa et al. deposited NiO_x films with (111) preferred orientation and are polycrystalline cubic structures. Spray-deposited films were reported to have a higher band gap compared to the chemical bath-deposited films [16]. An optical bandgap of 3.67 eV was reported by Desai in 2016 for NiO_x deposited from nickel nitrate precursor using the pneumatic spray pyrolysis technique. The film was found to have a cubic bunsenite crystal structure with rough topography. The richness of the film surface with oxygen compared to nickel was also observed [15]. Kim et al. NiO_x films prepared by the sol-gel method were investigated for their properties, with improvement in crystallinity reported on doping the NiO_x thin film with Cu. An increase in grain size from 38 nm to 50 nm on doping was also observed. Reduction in the band gap was seen in the doped film as compared to the undoped NiO_x, alongside the significant decrease in resistivity on doping from 320 □m to 23 □m [31]. The NiO_x film deposited by Kakherskyi et al. was found to be nanostructured, with uniform distribution of nickel and oxygen atoms, (111) and (222) planes were reported for reflections, but no reflection at (222) was observed for annealed films. Some carbon presence was observed that could be attributed to the decomposition of organics present in the precursor [14].

The reflectivity of NiO_x thin film on silicon was investigated by Jlassi et al., with the deposition on NiO_x thin film on silicon reported to be responsible for a drop in the reflection of silicon, with double-layered NiO_x film on the silicon substrates reported to exhibit the highest reduction in the reflectivity of the substrate, dropping significantly from 45% reflectivity to 15% reflectivity. A pyramid-like surface morphology was observed [13].

Using USP López-Lugo et al. deposited on glass substrates NiO_x film and Lithium-doped NiO_x thin film that is polycrystalline in nature, with the Li dopant effect not following a definite trend. The films are of low roughness in morphology, and p-type in nature [18].

2.6 Chemical spray pyrolysis method

Spray pyrolysis is a technique that involves the spraying of a precursor solution, containing atoms which is a representative of the desired compounds onto suitable substrates that are heated to a temperature sufficient for pyrolysis of the compound to occur [20].

It is an appealing option due to its versatility in thin film deposition, coupled with its suitability for deposition without being in a vacuum and the low cost associated with the use of the method [9]. The ability to use any substrate for deposition, large area deposition, and easy scalability for industrial application, alongside the cost factor was cited further as additional advantages of spray pyrolysis [36].

The spray pyrolysis method has been a popular technique for the deposition of thin films due to the relative ease of usage, and ability to influence the thickness and deposition rate of films by varying the spray parameters, hereby solving one of the challenges of the sol-gel technique [20].

An illustration of the typical setup is in Figure 5, showing the spray nozzle where the precursor mist passes through for spraying on a substrate. The metal plate sits on a heater that supplies the heat needed to attain the temperature needed for the formation of the film.

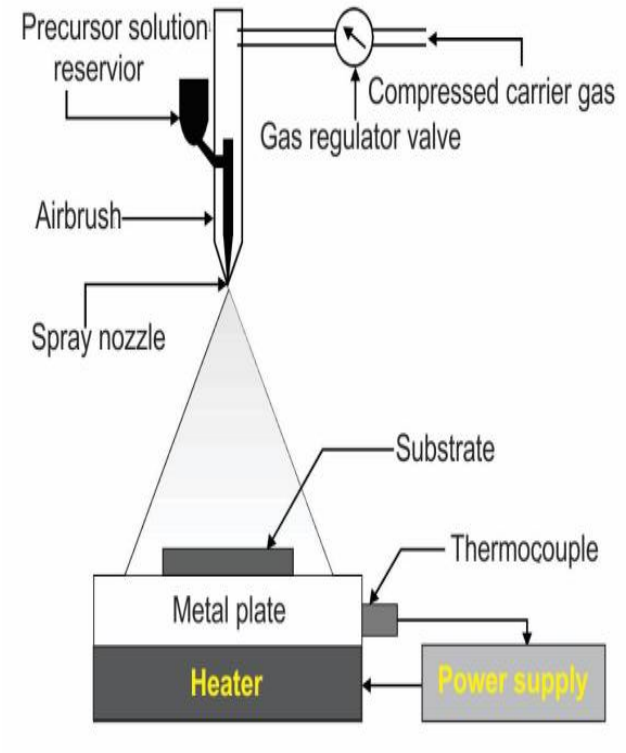

Figure 5. Schematic illustration of spray pyrolysis setup

2.6.1 Types of chemical spray pyrolysis method

There are several types of chemical spray pyrolysis methods and can be classified based on the type of atomizer in use. Fig 7 contains three popular types of chemical spray pyrolysis methods based on the form of atomization. The classification based on the atomization technique are:

- Pneumatic spray pyrolysis (PSP): This type of chemical spray pyrolysis involves the use of a pneumatic or airblast atomizer to produce an aerosol from the aqueous precursor. The diameter of each droplet made from the precursor solution is inversely proportional to the pressure of the solution and directly proportional to the air pressure released [37].

  The PSP system has a particle collector, an atomizer system, a pressure control system, and a reactor as part of its components. Its working principle involves the spraying of precursor solution through a pneumatic atomizer onto a substrate in a high-temperature reactor, with pyrolysis occurring to form a thin film [38].
- Electrostatic spray pyrolysis (ESP): This is a form of chemical spray pyrolysis where the spray nozzle generates highly positively charged spray at high voltage under electrostatic force. The droplets move across the electrostatic field towards the substrate on the hot plate, decomposing on it to form a coating. A schematic of the experimental setup of ESP is shown in Fig 6 detailing the components of the ESP. The components of ESP are the heater controlled by the thermocouple, a high-direct current voltage source, and a metal nozzle for transportation of the precursor solution through a syringe connection [37], [38].

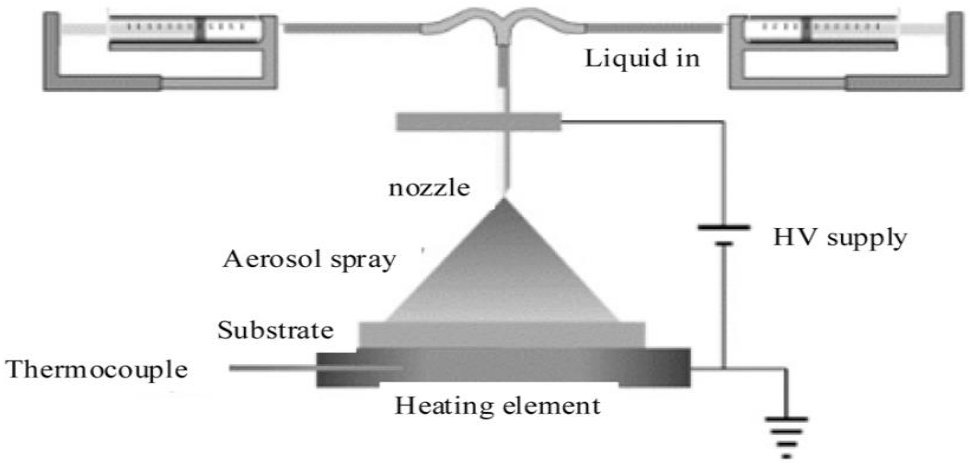

Figure 6. Electrostatic spray pyrolysis technique experimental setup [38]

- Ultrasonic spray pyrolysis (USP): Ultrasonic generator is used in transforming precursor solution into droplets as shown in Fig. 8. Ultrasound drives the

combination of the chemical components of the precursor inside the droplets, the compressed gas from the compressor sweeps across and carries the droplet with it as an aerosol. The solvent evaporates off the droplets in the USP reactor before the decomposition of the dry droplets [38].

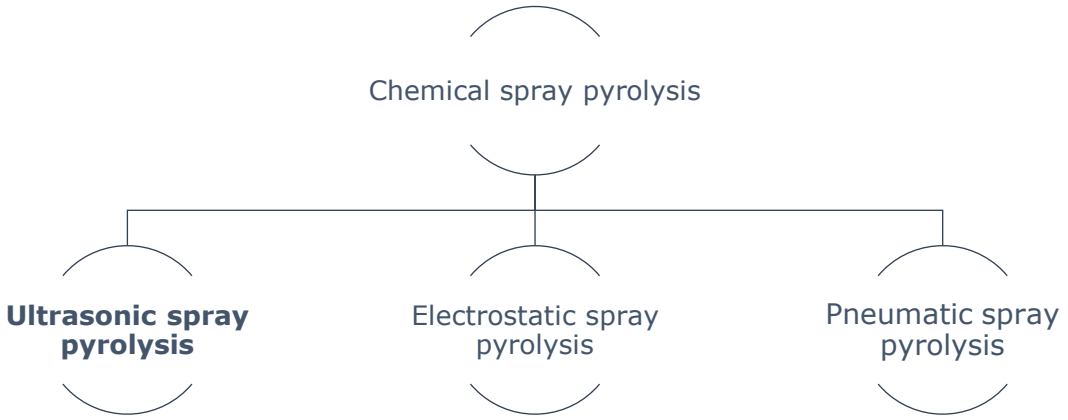

Figure 7. Types of chemical spray pyrolysis based on atomization techniques [37]

2.7 Ultrasonic spray pyrolysis

USP is a type of chemical spray pyrolysis, where an ultrasonic generator is used as an atomizer. The precursor solution when introduced to the chamber containing the ultrasonic generator is in aqueous form but becomes vaporized in the ultrasonic generator, forming droplets of a few microns in size. The ultrasonic generator atomizes the precursor solution into uniform fine mists employing ultrasonic power of 100W and at 2.56 MHz frequency [37].

These generated droplets that contain the precursors are transported by carrier gas through a channel or tube, through a nozzle onto the heated substrate.

Directory gas guides the movement of the aerosol as it sprays on the heated substrate. The heat from the heated substrate evaporates the solvent of the droplets as it journeys towards the substrate, initiating the pyrolysis process, with the metal oxide that is of interest forming a thin film on the substrate. It is a cost-effective and simple method and very useful for the deposition of metal oxide thin films.

The schematic in Fig 8 shows the basic components and steps involved in the use of USP for the deposition of a thin film. The precursor solution is introduced into the container fitted with an ultrasonic generator, where the solution is converted into fine droplets. The ultrasonic generator has piezo crystals that oscillate at high frequencies,

forming stationary waves within the solution in the container, leading to fast vaporization. The compressed gas (air) travels through the container and carries the droplets through a channel or tube in the form of an aerosol. The aerosol travels through the nozzle attached to the pipe or channel and is sprayed toward the heated substrate on the heater [20], [38].

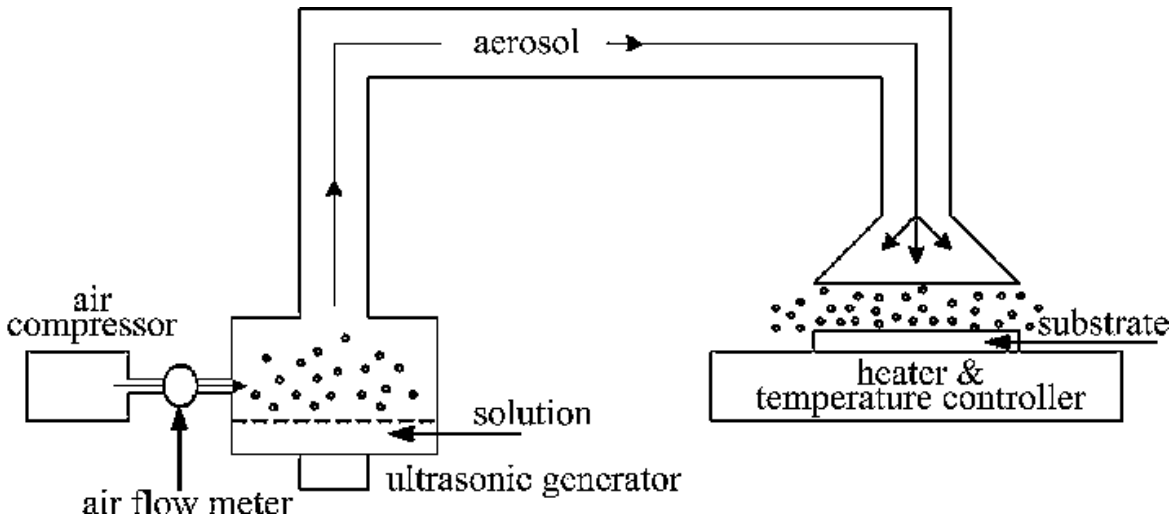

Figure 8. Schematics of Ultrasonic spray pyrolysis setup [7].

2.7.1 Advantages and disadvantages of ultrasonic spray pyrolysis

Table 2.2. Advantages and disadvantages of USP [20]

Advantages	Disadvantages
Smaller droplet size of precursor solution	Low yield
Thickness and deposition rate can be influenced easily by tweaking spray parameters	Possible oxidation of sulfides in air atmosphere
Low cost of operation compared to other techniques that require complex devices	The density of the fog is depended on the viscosity of the solution.
Easy scalability as it can be used on substrates irrespective of their quality in the absence of vacuum	
The operation temperature is moderate	
Changing the composition of the precursor solution can be used to vary composition	

gradients across the thickness of the film, making distinct layers	
Ease of usage and freedom with precursor solution makeup	
Easy to scale-up	

2.8 Applications of NiO_x thin films

Sajilal & Ezhil Raj deposited NiO_x thin films on Si substrate using CSP for application as electrochromic display devices [9]. NiO_x thin film deposited using spray pyrolysis with a perfume atomizer was investigated for its usage as electrodes in electrochromic devices and solar cells by Cattin et al. The authors noted that due to the inability of the films to sufficiently satisfy all the requirements for the earlier stated applications, they can still be of great use for gas sensor devices due to their high porosity [19]. Gomaa et al. deposited NiO_x thin film using CBD (chemical bath deposition) and CSP technique, with the CSP NiO_x suggested for application in invisible electronics [16]. Using the sol-gel synthesis technique to deposit NiO_x films and investigating it for its properties and application, Kakherskyi et al. found NiO_x nanomaterials as strong candidates for flexible oxide electronic and solar cells applications [14], using the same method Kim et al. investigated NiO_x for application in organic photovoltaic cells [31].

Layers of NiO_x thin films were deposited on a silicon substrate by Jlassi et al. using the sol-gel method and investigated for its possible application as an antireflection layer. Double layers of the film returned the best performance by reducing the percentage reflection of the silicon layer by two-thirds. The authors reported that increasing the layers further would have an opposing effect by increasing the reflectivity further but still less than the substrate reflection [13].

NiO_x and the lithium-doped thin films were explored for their application as a hole transport layer in optoelectronics, with lithium doping level reported to influence its optical and electrical properties. A successful application was found with its incorporation into LED [18]. It is also reported that NiO_x can find possible usage as electrodes in supercapacitor device applications [39].

2.9 Summary of the literature review

The summary of the review is as follows.

- NiO_x film, a p-type semiconductor with a wide bandgap between 3.5 and 4.3 eV has been of considerable interest due to its versatility in properties and how its properties can be modified through preparation parameters.
- The film has found various applications as a hole transport layer, gas sensor, flexible electronics, anti-reflection coating, optoelectronics, electrodes in electrochromic devices, and solar cells.
- NiO_x is a promising hole transport layer due to its chemical stability, favourable energy level matching, low cost of production, and high hole mobility.
- It has been deposited using a wide range of techniques, from sol-gel, chemical spray pyrolysis, chemical bath deposition, pneumatic spray pyrolysis, and to a lesser degree ultrasonic spray pyrolysis.
- Post-deposition annealing is a process usually employed to improve the crystallinity, electrical and optical properties of NiO_x thin films.
- USP is an interesting technique for the deposition of this film due to its cost-effectiveness, ability to be used in atmospheric conditions, simplicity, and ease of usage.

2.10 Aims of the thesis

The aims of the thesis are

- To acquire knowledge of ultrasonic spray pyrolysis techniques for the deposition of metal oxide thin films.
- To obtain knowledge on material (thin films) characterization techniques.
- To develop NiO_x thin films by ultrasonic spray pyrolysis (USP) technique and investigate the influence of USP deposition conditions, including the deposition temperature.
- To implement the use of the fuel (acetylacetone) in the precursor solution for the ultrasonic spray pyrolysis process.
- To represent and discuss the impact of post deposition treatment on the structural and optoelectronic properties of NiO_x films.
- To discuss the mechanism of physicochemical processes responsible for changes in the properties of the films depending on the deposition variables.

3. METHODOLOGY

3.1 Chemicals

The reagents used in the deposition of NiO_x thin film alongside the company they were sourced from, formula, and purity is stated in Table 3.1 below.

Table 3.1. Reagents used in the preparation of spray solution for NiO_x thin film deposition

Deposited thin film	Formula of the reagent	Reagent	Company	% Purity
NiO_x thin films	$NiNO_3.6H_2O$	Nickel (II) nitrate hexahydrate	Thermo Fisher Scientific	98
	C_2H_5OH	Ethanol (EtOH)		96
	$C_5H_8O_2$	Acetylacetone (AcAcH)	Acros Organics,	99+

3.2 Substrates preparation

2cm by 2cm (4-sq cm) borosilicate glass was cut from bulk as substrates. The substrates were ultrasonically cleaned at 50 ^oC in acetone, isopropyl alcohol, and distilled water for 10 minutes respectively. The substrates were dried in a jet of compressed air and placed in previously cleaned sample containers to prevent contamination ahead of their use in the spray deposition of NiO_x thin films.

3.3 Precursor spray solution preparation

A spray solution for reference sample of NiO_x thin film was prepared using nickel nitrate in ethanol, in the absence of any acetylacetone. Nickel nitrate and acetylacetone were mixed in ethanol for the other samples, with the acetylacetone acting as fuel to generate large amount of heat during the combustion process. The idea and procedure of using acetylacetone as a possible fuel in the preparation thin film was derived and modified from earlier reports [43], [44]. The NiO_x precursor solution was prepared by dissolving the addition of nickel (II) nitrate hexahydrate $NiNO_3.6H_2O$ and acetylacetone in 300 mL ethanol as shown in Fig 9.

Table 3.2. Preparation of spray solution

Sample	$NiNO_3$ amount/concentration	AcAcH amount/concentration	Ethanol	$NiNO_3$:AcAcH mole ratio
A1	2.7413g / 0.05M	309 µL / 0.01M	300 mL	5:1
A2	2.7431g / 0.05M	309 µL / 0.01M	300 mL	5:1
A3	2.7447g / 0.05M	309 µL / 0.01M	300 mL	5:1
A4	2.7418g / 0.05M	309 µL / 0.01M	300 mL	5:1
A5	2.7406g / 0.05M	309 µL / 0.01M	300 mL	5:1
B1	2.7409g / 0.05M	618 µL / 0.02M	300 mL	5:2
C1	2.7407g / 0.05M	927 µL / 0.03M	300 mL	5:3

Each sample solution was stirred in a beaker for approximately 15 minutes at room temperature to allow for homogeneous dissolution, resulting in a transparent, green-coloured solution. The synthesis was conducted by quantitatively mixing the two starting reagents of $NiNO_3.6H_2O$ (0.05 mol) and acetylacetone in 300 mL of ethanol from $NiNO_3$:AcAcH 5:1 mole ratio to 5:3 mole ratio depending on the sample solution being prepared as presented in Table 3.2. The deposition of the film commenced once the sample was sufficiently dissolved and formed a homogenous light green solution.

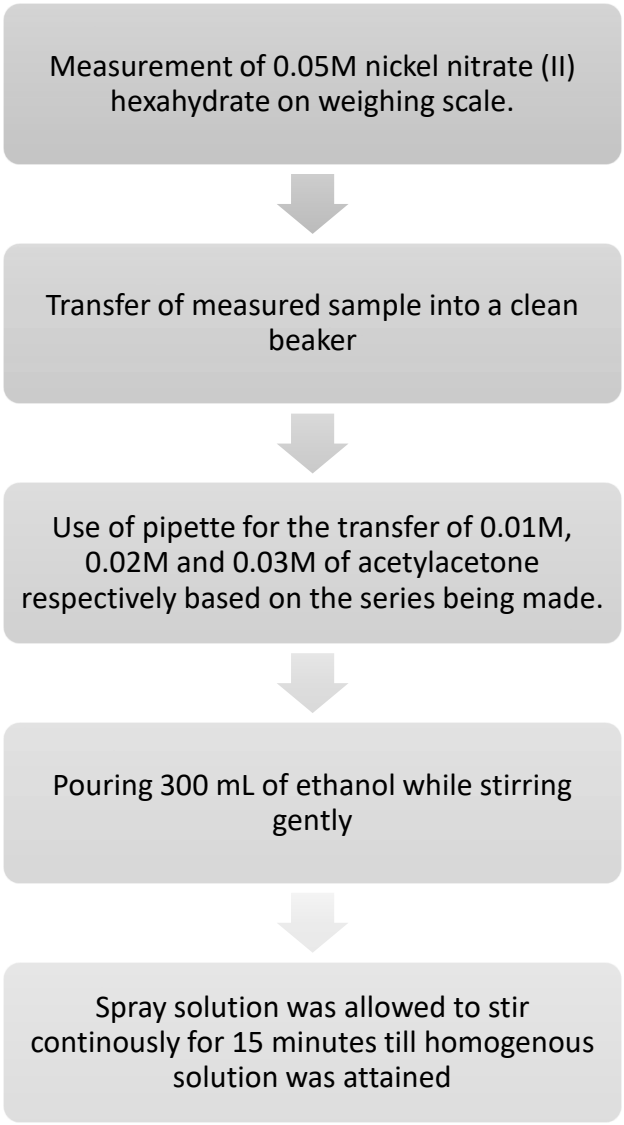

Figure 9. Flowchart illustrating the flow of the spray solution preparation.

3.4 USP apparatus and parameters

The ultrasonic spray pyrolysis setup as illustrated in Fig 10 uses an ultrasonic generator to convert the spray solution into an aerosol. The air flowmeter is used to regulate or control the flow of the directory and carrier gas, temperature controller to set the substrate temperature on the heater. A pipe is used as a form of a channel to transport the aerosol for spraying on the substrate.

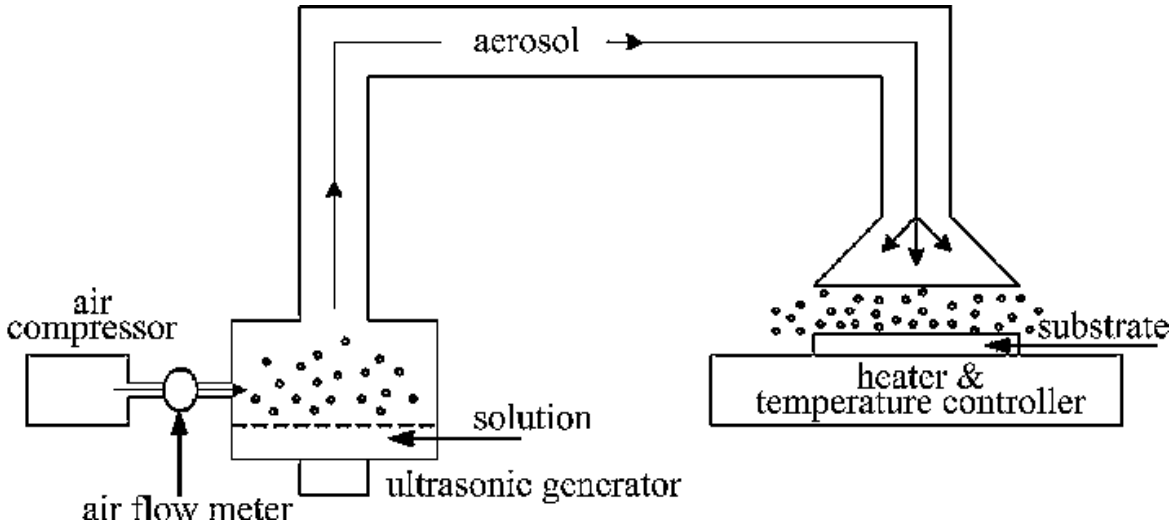

Figure 10. Experimental setup of USP [7] .

Parameters like carrier gas flow rate and directory gas flow rate, and substrate temperature highlighted in the deposition parameters of the NiO_x thin film were followed.

3.5 Deposition of NiO_x thin films

A reference sample was deposited at 400 °C using ethanolic solution of nickel nitrate, forming a black non-transparent film. In order to optimize the NiO_x thin film deposition from the $NiNO_3$:AcAcH mix, ultrasonic spray pyrolysis was used to deposit at different deposition conditions, first varying the temperature from 200 to 400 °C for the optimal temperature. The optimization was done further, varying the fuel content (acetylacetone) molar ratio from 1 to 3 molar ratio.

The prepared precursor solution was poured into the ultrasonic generator in preparation for the deposition process. The earlier cleaned, and labelled borosilicate glass substrates were placed on a marked area of the heater, and the deposition temperature based on the series being deposited was set using the temperature controller connected to the heating plate. On the system controlling the deposition, spray parameters were inputted, 4 steps being the deposition step used for the deposition of the NiO_x thin film. A total of 62 cycles was used per sample series for 300 ml solution.

Based on the series being deposited, the heater is allowed to attain the set temperature and allow to stabilize at the temperature, before the ultrasonic generator was turned on to drive the formation of aerosol for the spraying process. Directory gas flow rate of 0.9 L/min and carrier gas of 8 L/min were maintained on the gas flowmeter, for the direction of the spray target area and the carriage of the aerosol. The gas used for this

process is compressed air. The gas controller switch is turned on after all the conditions have been fulfilled and the ultrasonic generator has been turned on, hence kicking off the spraying of the aerosol onto the hot substrates. The precursor solution was loaded three times in portions of 100 mL per loading using a funnel. After the solution spraying was concluded, the substrates were allowed to cool down by themselves after turning off the gas controller alongside the ultrasonic generator. The temperature control was switched off to commence the gradual cooling of the samples. Furthermore, the samples were transferred into a cleaned, labelled sample container as soon as they have cooled totally.

The deposition parameters of NiO_x thin films as related to the different samples' series are compiled in Table 3.3.

Table 3.3. Deposition parameters of NiO_x thin films on borosilicate glass

Sample name	NiO_3:AcAcH molar ratio	Substrate temperature T_s (°C)	Deposition condition
A1	5:1	400	0.05M $NiNO_3$/0.01M AcAcH
A2	5:1	350	0.05M $NiNO_3$/0.01M AcAcH
A3	5:1	300	0.05M $NiNO_3$/0.01M AcAcH
A5	5:1	250	0.05M $NiNO_3$/0.01M AcAcH
A5	5:1	200	0.05M $NiNO_3$/0.01M AcAcH
B1	5:2	400	0.05M $NiNO_3$/0.02M AcAcH
C1	5:3	400	0.05M $NiNO_3$/0.03M AcAcH

The general parameter for all the series deposited is that the deposition condition is 4 steps and 62 cycles, with a directory gas flow rate of 0.9 L/min and 8 L/min maintained across all the samples. The deposition process took about 1 hour 40 minutes per deposition.

3.6 Annealing of NiO_x thin films

The NiO_x deposited on borosilicate glass substrates, both samples of the same mole ratio and differing temperature, and those of the same temperature and different mole ratio were annealed at 500 °C and 600 °C in the open air for 30 minutes using a Prazitherm laboratory oven.

A sample each from the deposited series was arranged on the heating plate of the hot plate, temperature set at 500 ^{o}C for the first batch of annealing using the temperature controller. The timer was started as the temperature regulator maintained 500 ^{o}C and the heater was switched off as the timer clocks 30 minutes. The samples were allowed to cool gradually before being transferred into neat, marked sample containers.

The same process was further repeated for the annealing of another batch of the deposited samples but at 600 ^{o}C. The same procedure was followed except for the temperature controller set at 600 ^{o}C. Samples were allowed to cool gradually and then transferred to marked sample containers, similar to what was done at 500 ^{o}C.

The NiO_x films made from $NiNO_3$:AcAcH 5:3 were annealed in an ampoule using Carbolite Gero EZS 1200 furnace, the films were arranged in the furnace, with annealing temperature set at 400 ^{o}C and 500 ^{o}C for 30 minutes each. The films were allowed to cool in the furnace gradually. In Table 3.4 lies the conditions and the corresponding samples treated.

Table 3.4. Annealing conditions of NiO_x thin films for 30 minutes per series

Sample	**$NiNO_3$:AcAcH molar ratio**	**T_{asd} (^{o}C)**	**T_{ann} (^{o}C)**
A1	5:1	400	500
			600
A2	5:1	350	500
			600
A3	5:1	300	500
			600
A4	5:1	250	500
			600
A5	5:1	200	500
			600
B1	5:2	400	500
			600
C1	5:3	400	500
			600

3.7 Characterization methods

3.7.1 UV-Vis spectroscopy

Jasco V-670 spectrophotometer was used to investigate the optical properties of the deposited thin films at 250 to 1500 nm range using a 60 mm ϕ integrate sphere. The total reflectance and total transmittance of both as-deposited and annealed NiO_x thin films deposited on the borosilicate glass substrates were measured. The results of the optical measurement were used to derive the optical bandgap of the thin films by plotting the tauc plots for each of them. $BaSO_4$ was used as an ideal white body, air as a reference with a scan speed of 400 nm/min for the measurement.

3.7.2 X-ray Diffraction

Using X-ray diffraction (XRD), the NiO_x thin films deposited on borosilicate glass substrates were investigated for their structural properties using a Rigaku Ultima IV diffractometer. The diffractometer was used to record XRD patterns with Cu Kα radiation (λ = 1.5406 Å, 40 kV at 40 mA). Rigaku PDXL software, using data card JCPDS 01-080-5508 was used to analyze the XRD data of NiO_x thin films deposited.

A scan speed of 5°/min, a scan range of 30 to 80°, and a sampling width of 0.02° on a 2-theta configuration were used for the measurement of the structural properties of the films. The mean crystallite size was derived using the Scherrer method, from the full width at half maximum (FWHM) of the NiOx bunsenite phase at (200) peak.

3.7.3 Van der Pauw measurement

The Van der Pauw measurement was conducted using the four points probes method on MMR's Variable Temperature Hall System with Van der Pauw controller H-50. Indium was used as the electrode material for the four points.

The effect was observed under the combination of the magnetic field through the thin film and current along the length of the thin film, creating an electrical current that is perpendicular to both the current and magnetic field, further creating a transverse voltage that is perpendicular to both the current and magnetic field [40]. The contacts were made at the corners of the sample's square geometry using indium.

3.7.4 Scanning electron microscopy

The films were scanned using a high-energy beam of electrons to produce images of the film by SEM. Electrons accelerate down from the electron gun situated at the top of the column, passing through slits and lenses. This passage produces a focused beam of electrons, which is directed onto the surface of the thin film, and mounted on a stage in the chamber for analysis. The interactions of the beam of electrons lead to the production of backscattered electrons, secondary electrons, and characteristic X-rays which are picked up by detectors to form an image representing the sample characteristics [41].

Zeiss HR-SEM MERLIN with GEMINI II column is the scanning electroscope used to investigate the structural properties of the thin film.

4. RESULTS AND DISCUSSIONS

This chapter presents the results and discussions on the development of NiO_x thin films by USP deposition technique providing detailed analysis of changes in the structural, optical, and electrical properties of the films, depending on the chemistry of the USP precursors solution, deposition parameters, and post-deposition treatment conditions. Section 4.1 addresses the effect of USP deposition temperature and precursor molar ratio on the properties of NiO_x thin films. Section 4.2 reports the influence of post-deposition treatment (PDT) on the properties of the NiO_x thin films. The mechanism of the physicochemical processes that bring about the observed changes in the NiO_x thin films under investigation was dedicated to section 4.3 of this chapter.

4.1 Effect of USP deposition temperature and precursor molar ratio on the properties of NiO_x thin films

A series of samples were deposited to investigate the influence of NiO_x deposition conditions on the optical, structural, and electrical properties of the NiO_x hole transport layer. Section 4.1.1 addresses the impact of the deposition parameters on the optical properties of the NiO_x thin films deposited by USP. Section 4.1.2 reports on the effect of USP deposition parameters on NiO_x thin film structural properties. The electrical properties of the film were reported in section 4.1.3, showing the effect of the USP deposition parameters on the electrical properties of the film.

4.1.1. Total transmittance and optical band gap of NiO_x thin films

The optical properties of NiO_x layers were evaluated using UV-Vis spectroscopy. The total transmittance, of NiO_x thin film deposited onto borosilicate glass substrates is shown in Figure 11a indicating the effect of substrate temperature on the film transmittance. The substrate temperature varied between 200 ^oC and 400 ^oC, the impact of which was illustrated in Figure 11a. It can be observed that NiO_x films deposited at 200-300 ^oC exhibit 85 to 90% total transmittance. The increase of the substrate temperature to 350 ^oC slightly drops the transmittance of the layers to 80%. At 400 ^oC deposition temperature, the total transmittance of the films significantly decreased to 60% suggesting that this temperature generates significant changes in the optical bandgap of the NiO_x films.

Having noticed that 400 °C is the turning point in the total transmittance trend of the NiO_x films, in the next step the $NiNO_3$:AcAcH ratio in the USP precursor varied from 5:1 to 5:3 and its impact on the total transmittance of the layers was analysed. Figure 11b shows the effect of precursor molar ratio on the total transmittance of USP NiO_x thin films deposited at 400 °C. A slight increase in the transmittance of NiO_x film can be observed as the molar ratio of acetylacetone content of the precursor increases from 1 to 3. At the 5:1 $NiNO_3$:AcAcH molar ratio, the transmittance was just below 60 %, increasing to 60 % at the 5:2 $NiNO_3$:AcAcH molar ratio, and around 70% - for the 5:3 $NiNO_3$:AcAcH molar ratio.

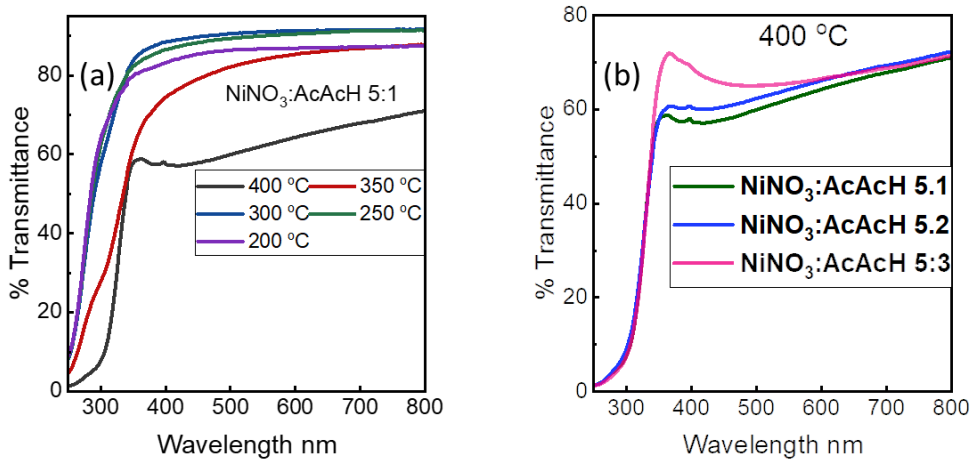

Figure 11 Effect of (a) substrate temperature and (b) $NiNO_3$:AcAcH molar ratio in the precursor solution on total transmittance of NiO_x thin films deposited by USP at 400 °C.

The bandgaps of the NiO_x films were determined from the total transmittance and total reflectance data sourced from the UV-Vis spectroscopy analysis conducted on the film. The bandgap was deduced by using the Tauc plot relation [17]:

$$\alpha(h\nu) = A\left(h\nu - E_g\right)^m \qquad (4.1)$$

where

□- the absorption coefficient,

hν- the photon energy,

E_g- optical band gap, eV.

m- constant (m=1/2 for allowed direct transitions, m=2 for allowed indirect transition). m characterizes the allowed electronic conversion of light absorption,

A= constant and does not depend on energy.

Direct band gap was assumed for the NiO_x thin film deposited on the borosilicate glass substrates, with the equation above in eqn 1 rewritten as:

$$(\alpha h\nu)^2 = A^2(h\nu - E_g) \qquad (4.2)$$

The optical band gaps of the NiO_x thin films were determined by extrapolating the linear part of the (□hv)^2 plot against photon energy hv as shown in Fig 12a [8].

The bandgaps of the films deposited decrease as the mole ratio of the acetylacetone component of the precursor solution increases, illustrated in Fig 12a and b. The bandgap values recorded are 3.61, 3.58, and 3.53 eV respectively for the 5:1, 5:2, and 5:3 NiO_x films are shown in Table 4.2. This can be attributed to the increasing crystallinity of the films as the mole ratio increases.

Fig 12b illustrated the decrease in the bandgap of the NiO_x thin film from 3.61 eV to 3.53 eV as the mole ratio of the acetylacetone component of the NiO_x thin film precursor solution increases. The effect of temperature on the optical bandgap of the thin films was exhibited in Fig 12c where there was little to noticeable difference in the bandgaps of the thin films deposited between 200 to 350 ^oC at around 4.3 eV. A sharp drop in optical bandgap was observed as the substrate temperature increased from 350 to 400 ^oC, culminating in a bandgap of 3.61 eV. Data on this effect is presented in Table 4.1. Data presenting the drop in bandgap observed on increasing the precursor mole ratio of the NiO_x films are stated in Table 4.2.

Table 4.1 Effect of temperature on the bandgap value of NiO_x thin film deposited from $NiNO_3$:AcAcH=5:1 molar ratio in the precursor solution.

$NiNO_3$:AcAcH molar ratio	**Deposition temp. ^oC**	**Bandgap eV**
5:1	400	3.61
5:1	350	4.26
5:1	300	4.31
5:1	250	4.32
5:1	200	4.28

Table 4.2 Effect of $NiNO_3$:AcAcH molar ratio in the precursor solution on the NiO_x bandgap

$NiNO_3$:AcAcH molar ratio	**Deposition temp. ^oC**	**Bandgap eV**
5:1	400	3.61
5:2	400	3.58
5:3	400	3.53

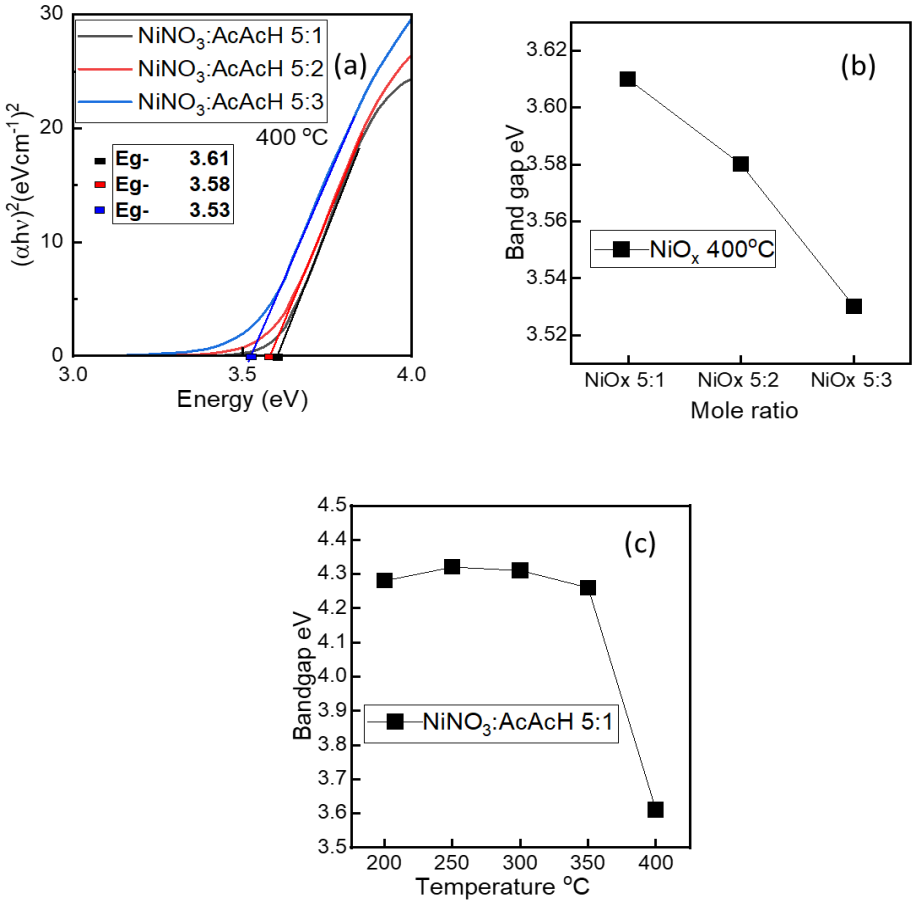

Figure 12. (a) Tauc plot of NiO_x thin films deposited on borosilicate glass at 400 °C from different $NiNO_3$:AcAcH molar ratios. (b) Evolution of the bandgap value with the variation of the $NiNO_3$:AcAcH molar ratio from 5:1 to 5:3 in the precursor solution. (c) Effect of USP deposition temperature on the bandgap of NiO_x deposited from the precursor containing $NiNO_3$:AcAcH=5:1 molar ratio.

4.1.2. Structural properties of NiO_x thin films

The crystal structure of the NiO_x thin films deposited by USP onto borosilicate glass substrates was examined by the X-ray diffractometry method. The films deposited at 200-300 °C showed poor crystallinity structure with a significant amount of amorphous phase. Deposition at 350 °C resulted in the clear appearance of (111) and (200) XRD peaks, assigned to bunsenite crystal structure with 225:Fm-3m space group symmetry (JCPDS 01-080-5508) in agreement with peaks reported in other literature [32], [39]. A further increase of the substrate temperature to 400 °C resulted in increased intensity of (111) and (200) XRD peaks together with the appearance of (220) peak. The sharpness of the peaks indicates to significant improvement in the crystalline quality of the NiO_x films deposited at 400 °C.

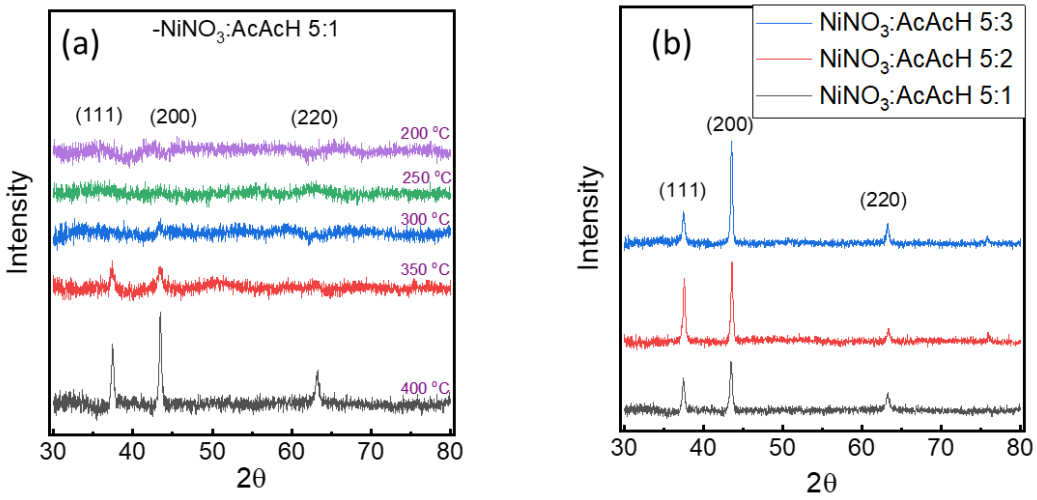

Figure 13. XRD patterns of NiO_x thin film showing the (a) Impact of substrate temperature on the film (b) Impact of mole ratio on the film.

The impact of the $NiNO_3$:AcAcH molar ratio in the precursor solution on the crystal structure of NiO_x deposited at 400 °C is shown in Figure 13b.

Maintaining the same deposition temperature at 400 °C while varying the $NiNO_3$:AcAcH molar ratio in the precursor, there was a mixed effect on the (111) diffraction peak with the peak getting stronger for the NiO_x films deposited from $NiNO_3$:AcAcH of 5:2 before dropping in intensity at 5:3 as shown in Fig 13b. A clear trend was observed with the effect of increasing the $NiNO_3$:AcAcH molar ratio on the (220) diffraction planes of the bunsenite phase. The intensity of the bunsenite peak (220) gradually increased in the deposited film as the mole ratio increases from $NiNO_3$:AcAcH 5:1 to 5:3, finalizing in a very sharp peak, with increased crystallite size which can be attributed to improvement in quality. The increase in crystallinity attributed to the increase in concentration is consistent with earlier reports [39].

The crystalline films deposited have more than one diffraction plane, making them polycrystalline in nature, as was reported by other researchers [32]. The crystallite sizes of the films increased with increasing temperature as shown in Table 4.3 and a similar outcome was recorded for increasing mole ratio, aligning with observations made in some papers addressing NiO_x [32].

Table 4.3. Average crystallite size, Full width half maxima, and lattice constant of NiO_x thin film of different precursor mole ratio

$NiNO_3$:AcAcH molar ratio	Temp (°C)	Phase	Crystallite size (nm)	FWHM at 200 plane (°)	Lattice constant a (nm)
5:1	200	Amorphous	-	-	
	250	Amorphous	-	-	
	300	Amorphous	-	-	
	350	Crystalline	16.1	0.556	0.41524
	400	Crystalline	26.0	0.343	0.41573
5:2	400	Crystalline	30.0	0.298	0.41501
5:3	400	Crystalline	32.4	0.276	0.41552

The FWHM of the thin films decreases from 0.556 to 0.323 as the temperature of the substrates increases from 350 °C to 400 °C. A similar effect was observed as an increase in the mole ratio of the AcAcH portion of the precursor from 1 to 3 mole, the FWHM decreases from 0.343 to 0.276. In both observations earlier stated, the crystallite size increased from 16.1 nm to 32.4 nm as the temperature and mole ratio increased as shown in Table 4.3.

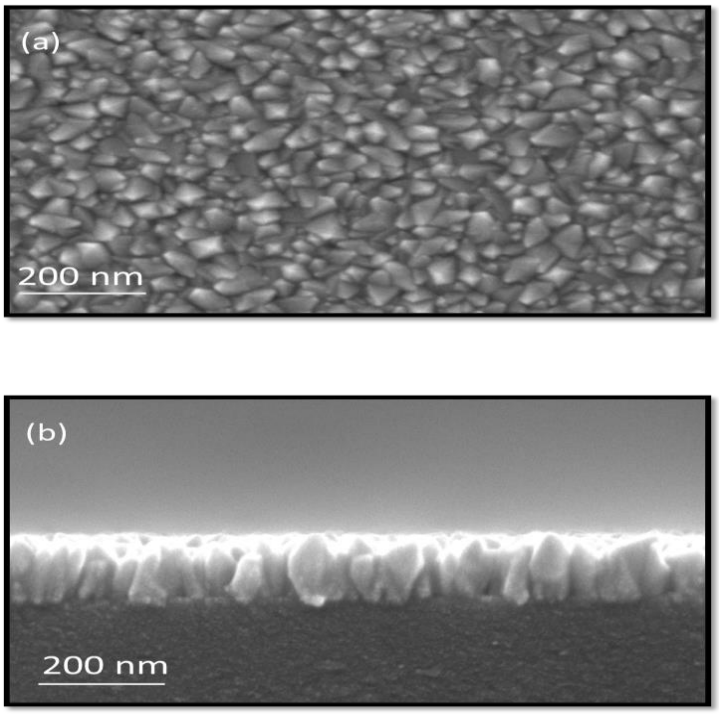

Figure 14. SEM images showing the (a) top view (b) cross-sectional view NiO_x thin film

The morphology of NiO_x thin films deposited by USP was investigated further by using scanning electron microscopy. The top-view and cross-section SEM images of the film made from $NiNO_3$:AcAcH 5:3 are shown in Figures 14a and b respectively. The thickness of the film was found to be 114 nm. The film has a vertically oriented growth, with flat and rounded edges, and loosely packed grains. It can be observed that NiO_x film forms cubic polycrystals on the borosilicate glass layer, which are uniform in nature. There are some gaps amongst crystals in the as-deposited film as shown in Figures 14a and b.

4.1.3. Electrical properties

Table 4.3 Van der Pauw measurements of NiO_x thin film

Conditions	$NiNO_3$:AcAcH Molar ratio	Resistivity (Ωcm)	Sheet resistance ($Ω/cm^2$)
As deposited at 400 °C	5:1	1.1×10^5	1.4×10^9
	5:2	8.4×10^4	1.1×10^9
	5:3	3.9×10^6	4.9×10^{10}

Table 4.4 presents the impact of the precursor mole ratio on the resistivity of NiO_x thin film. NiO_x thin film made with $NiNO_3$:AcAcH 5:1 has a resistivity of 10^5 Ωcm and sheet resistance of 10^9 $Ω/cm^2$, with a slight decrease in resistivity to 10^4 Ωcm for $NiNO_3$:AcAcH 5:2 thin film. The resistivity increased to 10^6 Ωcm for the film made with $NiNO_3$:AcAcH 5:3 precursor mix, which can be linked to more organic from the 3-mole ratio of acetylacetone in the NiO_x thin film precursor. The sheet resistance of the films is in a similar range to the order of 10^9 apart from NiO_x thin film in 10^{10} order of sheet resistance for $NiNO_3$:AcAcH 5:3.

4.2. Influence of post-deposition treatment on the properties of NiO_x thin films

The impact of post-deposition treatment on the deposited NiO_x thin film optical, structural, and electrical properties was examined in this section. Item 4.2.1 addresses the optical properties of the post-deposition treated NiO_x thin films and the impact of post-deposition treatments on the properties. Item 4.2.2 reports on the effect of post-deposition treatments on NiO_x thin film structural properties. The electrical properties of the film were reported in Item 4.2.3, showing the effect of post-deposition treatments on the electrical properties of the film.

4.2.1 Total transmittance and optical band gap of NiO_x thin films after post-deposition treatments

The total transmittance for the three different mole ratios thin film as deposited at 400 °C and annealed in air at 500 and 600 °C as indicated in Figure 15a to c. The impact of annealing at the conditions earlier stated on the total transmittance of the films was analysed. It can be observed that NiO_x films of $NiNO_3$:AcAcH 5:1, both as-deposited and annealed at 500 °C and 600 °C are between 55 to 60 % total transmittance as shown in Fig 16a. Annealing of the $NiNO_3$:AcAcH 5:1 film showed a decrease in transmittance as the annealing temperature increases from 500 °C to 600 °C. Annealing of $NiNO_3$:AcAcH 5:2 film posted almost the same transmittance as the as-deposited film, as the difference is so close. The effect of annealing was more evident in films made from $NiNO_3$:AcAcH 5:3 precursor mix, with the as-deposited film having around 70% transmittance which reduce significantly to around 65% after annealing at 500 °C, dropping further when annealed at 600 °C to around 60%.

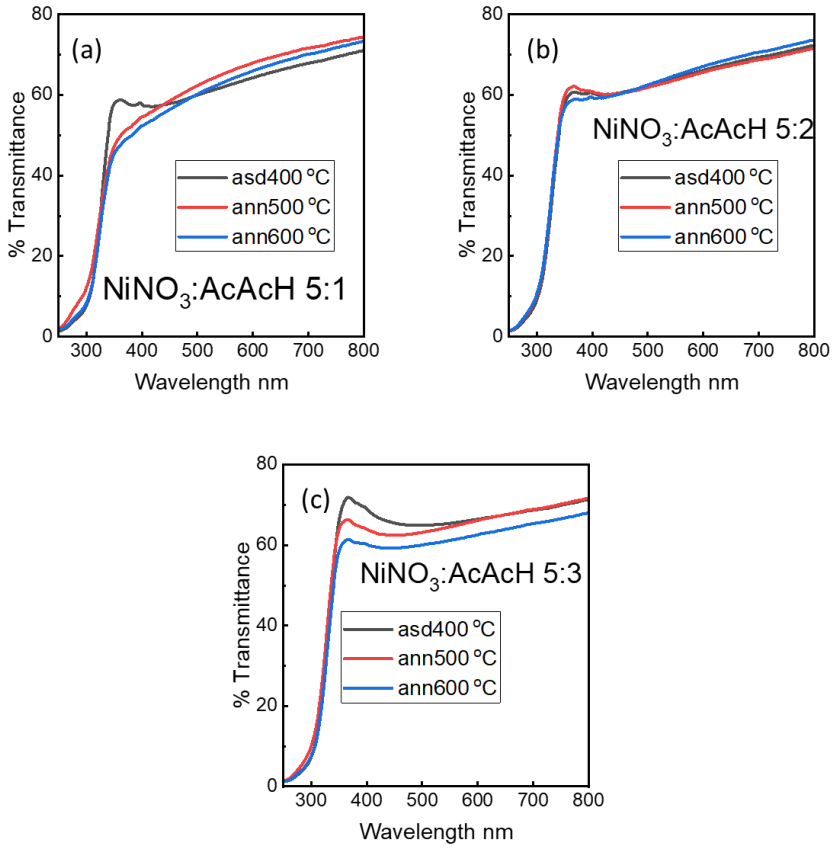

Figure 15. Impact of annealing at different temperatures on the transmittance of (a) $NiNO_3$:AcAcH 5:1 (b) $NiNO_3$:AcAcH 5:2 (c) $NiNO_3$:AcAcH 5:3 thin films

The decrease in optical transmittance on annealing can be related to increased surface roughness which in turn improves the diffusion of light.

The influence of annealing on the bandgap yielded a mixed result, without a clear trend on the impact of annealing on the bandgap as shown in Table 4.5. Overall, the bandgaps were slightly increased at the two annealing temperatures compared to the as-deposited film.

Table 4.4. Impact of annealing on NiO_x bandgap

Sample name	$NiNO_3$:AcAcH molar ratio	Dep. Temp., °C	Band gap as deposited (eV)	Band gap annealed 500 °C (eV)	Band gap annealed 600 °C (eV)
A1	5:1	400	3.61	3.72	3.67
A2	5:1	350	4.26	-	-
A3	5:1	300	4.31	-	-
A4	5:1	250	4.32	-	-
A5	5:1	200	4.28	-	-
B1	5:2	400	3.58	3.58	3.65
C1	5:3	400	3.53	3.58	3.54

4.2.2 Structural properties

The structural properties of the post-deposition treated NiO_x thin films were assessed for the impact of PDTs on them. SEM and XRD were the technique employed for the characterization. Table 4.6 presents the data on the effect of post-deposition treatments on NiO_x thin film. $NiNO_3$:AcAcH 5:1 film has a crystallite size of 26nm in its deposited form, on annealing in the open air at 500 °C, the crystallite size reduces to 24.1 nm and increased to 26.6 nm after annealing at 600 °C. NiO_x film made from $NiNO_3$:AcAcH 5:2 experienced a decrease in crystallite size from 30 nm to 28 nm on annealing at 600 °C. A similar effect was experienced for $NiNO_3$:AcAcH 5:3 as the crystallite size decreased from 32.4 nm to 31.4 nm after annealing at 600 °C. On annealing, there is a clear trend of decreasing crystallite size for the three NiO_x thin film samples under observation as the temperature increases.

The effect of annealing on the crystal structure of the NiO_x films was presented in Fig 16. The XRD pattern of $NiNO_3$:AcAcH 5:1 film was shown in Fig 16a, with the intensity of the peaks (111), (200), and (220) shown to remain almost the same post-annealing. In Fig 16b, $NiNO_3$:AcAcH 5:2 films showed (200) and (220) peaks intensity remaining the same as the deposited film, with a sharp increase in intensity observed on the (111) peak at 600 °C annealing temperature. The intensity of the peaks showed no evident

changes pre and post-annealing of the $NiNO_3$:AcAcH 5:3 thin films as shown in Fig 16c, indicating annealing of the film at this stage does not improve the quality of the film further.

Table 4.6. Influence of annealing on the crystals structure NiO_x thin film obtained from XRD analysis.

$NiNO_3$:AcAcH molar ratio	**Annealing**	**Temp (°C)**	**Phase**	**Crystallite size (nm)**	**FWHM**	**Lattice constant a(nm)**
5:1	-	400	Crystalline	26.0	0.343	0.41573
	Yes	500	Crystalline	24.1	0.370	0.41501
	Yes	600	Crystalline	26.6	0.336	0.41519
5:2	-	400	Crystalline	30.0	0.298	0.41501
	Yes	500	Crystalline	30.3	0.295	0.41459
	Yes	600	Crystalline	28.0	0.319	0.41493
5:3	-	400	Crystalline	32.4	0.276	0.41552
	Yes	500	Crystalline	31.3	0.285	0.41494
	Yes	600	Crystalline	31.4	0.284	0.41508

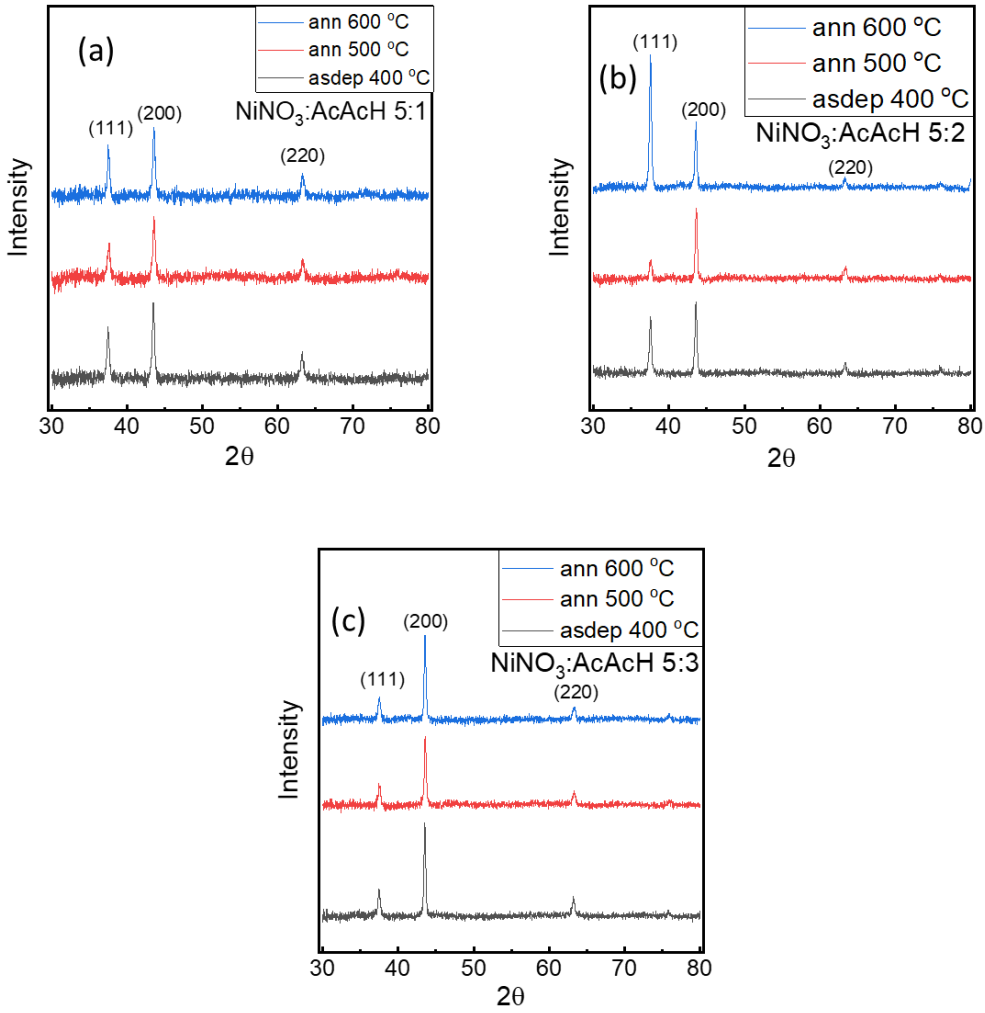

Figure 16. XRD patterns showing the impact of annealing at different temperatures on NiO_x thin film of (a) $NiNO_3$:AcAcH 5:1 (b) $NiNO_3$:AcAcH 5:2 (c) $NiNO_3$:AcAcH 5:3 and deposited at 400 °C.

The morphology of the films after post-deposition treatments on the films was investigated further using SEM. In Fig 17 the effect of annealing on the NiO_x film was addressed, with Fig 17a and b showing the top view and cross-sectional view of the deposited thin film at 400 °C substrate temperature while Fig. 17c and d showing the top and cross-sectional view of the annealed film in the open air at 500 °C. The images in Fig 17b and d show the as-deposited and annealed films on a layer of glass. It can be observed that NiO_x films form cubic polycrystals on the borosilicate glass layer, which are uniform in nature. There are some gaps amongst crystals in the deposited film as shown in Fig. 17a and b, reducing on annealing in the open air at 500 °C to form fused and more compact grains as shown in Fig. 17c and d.

It can be assumed that the annealing of the film increased the quality of the NiO_x thin film.

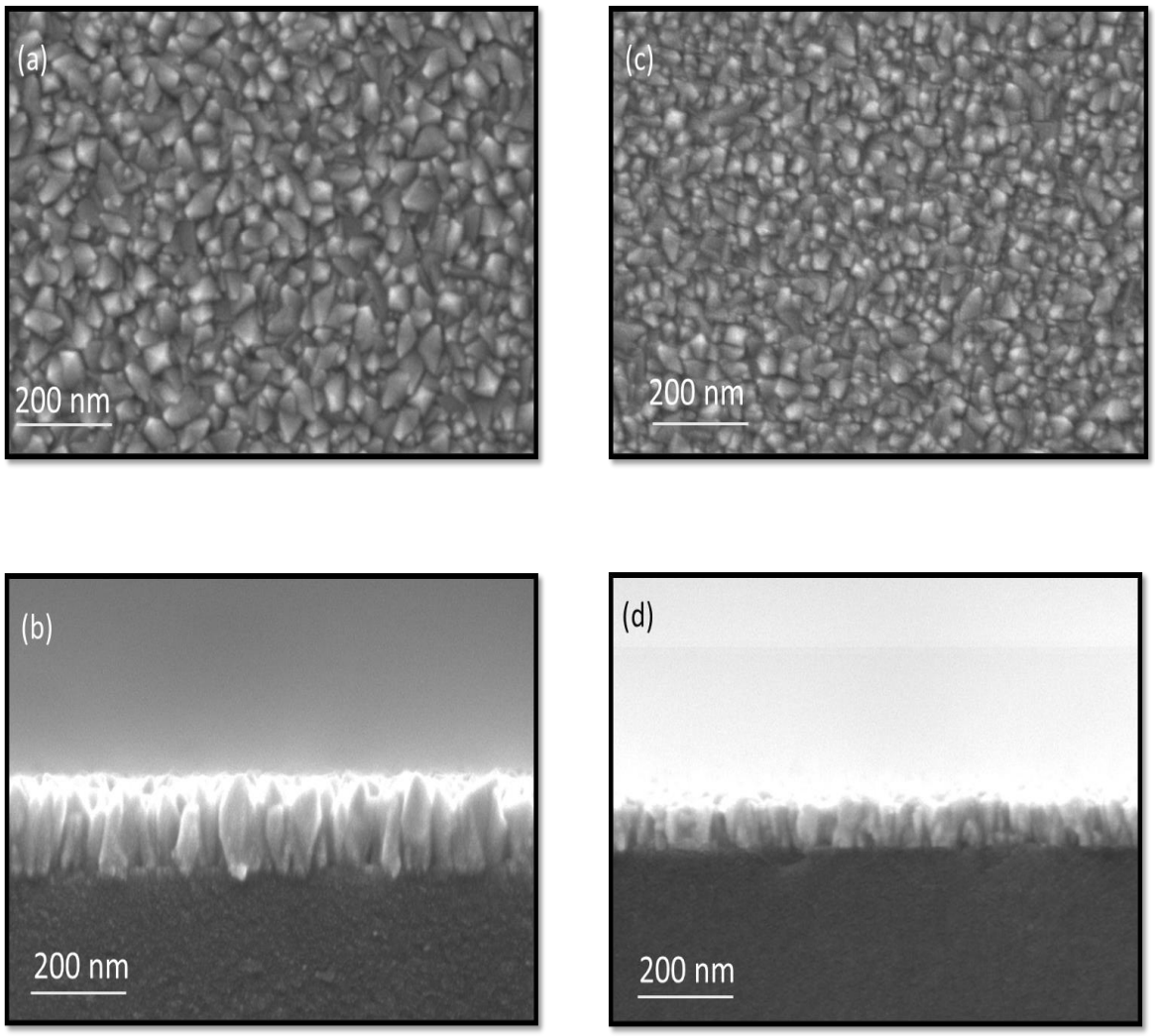

Figure 17. SEM images of NiO_x made from $NiNO_3$:AcAcH 5:3 (a) top view of as-deposited at 400 ^oC (b) cross-section of as-deposited at 400 ^oC (c) top view of annealed in the open air at 500 ^oC (d) cross-section of film annealed at 500 ^oC

The thickness of the as-deposited thin film was found to be 114 nm from the SEM image and 57 nm for the annealed film, with increased compactness and quality. This indicates that the PDT of NiO_x thin film led to a decrease in the thickness of the HTL, growing more compact.

4.2.3 Electrical properties

The data derived from the Van der Pauw measurement of pre and post-annealed NiO_x thin films are shown in Table 4.7. The annealed NiO_x thin films were evaluated for their resistivity and the results are presented in Table 4.7. For NiO_x 5:1 thin film, the resistivity of the film was within the same range as the deposited one but a drop in resistivity is observed at 600 ^oC annealing condition in air. Annealing NiO_x thin film of

$NiNO_3$:AcAcH 5:2 has no clear influence on its resistivity, with the resistivity staying within the same range of 10^5 Ωcm and increasing further to 10^5 Ωcm at 600 °C annealing temperature. There is a clear trend in the reduction of the resistivity of NiO_x of $NiNO_3$:AcAcH 5:3 from the order of 10^6 to 10^5 and 10^4 at 600 °C. The sheet resistance of the films stayed constant in the order of 10^9.

Table 4.7 Van der Pauw measurement of NiO_x thin films

Conditions	Molar ratio	Resistivity (Ωcm)	Sheet resistance (Ω/cm²)
As deposited	5:1	1.1×10^5	1.4×10^9
	5:2	8.4×10^4	1.1×10^9
	5:3	3.9×10^6	4.9×10^{10}
Annealed 500 °C in air	5:1	1.6×10^5	2.0×10^9
	5:2	5.2×10^4	6.5×10^8
	5:3	4.5×10^5	5.7×10^9
Annealed 600 °C in air	5:1	5.3×10^4	6.6×10^8
	5:2	4.5×10^5	5.7×10^9
	5:3	2.4×10^4	4.7×10^9

Doping of the NiO_x thin film with lithium has been reported to reduce the resistivity encountered in plain NiO_x film. The doping of the film was shown to lead to higher film quality and lower resistivity as increased availability of lithium atoms to replace the nickel atoms sites and increased hole concentration [25].

4.3. Mechanism of changes in the properties of NiO_x thin films depending on the deposition and post-deposition treatments conditions

According the results presented above, as deposited NiO_x thin films deposited by USP at 200-350 °C from 5:1 $NiNO_3$:AcAcH molar ratio in the precursor, contains high amount of amorphous phase and are characterized by wide band gap (~4,3 eV), high transparency (~80%), and high resistivity. Deposition from the same precursor solution at 400 °C resulted in crystalline NiO_x films with band gap (~3.6 eV), total transmittance of ~60% and resistivity of ~10^5 Ωcm. By changing the $NiNO_3$:AcAcH molar ratio in the precursor from 5:1 to 5:3, and applying post deposition treatments in air at 500-600 °C, little changes have been observed in the total transmittance of the NiO_x films (and corresponding band gaps), however noticeable changes were observed in crystallite size and resistivity of the films. The question is which mechanisms are behind the processes leading to these changes. Considering the conditions of the experiments, an increase AcAcH amount in the precursor solution leads to more fuel for the combustion process at the stage of the NiO_x film deposition by USP at 200-400 °C in air. The same process is present in the second stage, during the recrystallization of the films in the subsequent

PDT treatments steps in air at 500-600 °C. The PDT process in air is more intensive, in which the partial pressure of oxygen P(O_2) practically remains constant (considering the open atmospheric conditions), whereas the partial pressures of CO_2 and H_2O can significantly increase by increased temperature of AcacH-assisted combustion process [43]. It is likely that a higher temperature and higher CO_2 partial pressures can raise oxygen chemical potentials that can lead to a reduction of the concentration of oxygen vacancies [V_{O2}] and increase in the concentration of nickel vacancies [V_{Ni}]. It is well established that vacancy-type mechanism as a predominant disorder in the NiO_x films with [V_{Ni}] as the main responsible defect for p-type conductivity of NiO_x films. The mechanism for formation of defects within the NiO_x lattice that led to generation of holes are presented in [25]. An increase in the concentration of [V_{Ni}] should result in enhanced density of hole density in NiO_x and thus decrease the resistivity of the films. This phenomenon can explain the slight decrease of the resistivity of the layers in table 4.7. At the same time, looking at the variation of the resistivity when increasing the amount of AcacH amount in the precursor solution, for some cases the resistivity increases by almost half order of magnitude, implying that there is a concomitant effect of defect compensation effect. One possible explanation for this effect could be the incorporation of carbon impurity into the NiO_x lattice and probably its accumulation at the grain boundaries. Such processes are very common in metal-oxides deposited by USP in air [43]. Incorporation of carbon atoms into the lattice of NiO_x can occur through a substitutional mechanism at the oxygen sites or by taking an interstitial site [25]. Thus, the carbon impurity may introduce localized states through which the electrons or holes are trapped and thereby, decreasing the overall carrier concentration and hence increase the resistivity of the films. However, to prove this mechanism additional advanced measurements techniques such as XPS and SIMS analysis should be performed.

So, far these results show that USP technique is a feasible processing route with many degrees of freedom in optimization of deposition parameters suitable for fabrication of high quality, dense and uniform NiO_x films with reasonable optoelectronic properties. To apply NiO_x thin films as a hole transport material in thin film solar cells, implementation of doping strategies (to improve the electrical properties of the NiO_x films) represent an important challenge to be addressed in the future.

CONCLUSIONS

It was acquired the knowledge of ultrasonic spray pyrolysis techniques and obtain knowledge on material (thin films) characterization techniques UV-Vis, SEM, XRD, and van der Pauw was obtained during the course of the research.

It was successfully deposited NiO_x thin films using ultrasonic spray pyrolysis technique and it was investigated the influence of USP deposition conditions, including the deposition temperatures from 200 to 400 ^oC, with 400 ^oC emerging as the optimal temperature for the deposition of NiO_x thin film from the nickel nitrate and acetylacetone precursor mixture.

It was practically used the fuel idea into the chemical spray deposition method using acetylacetone in varied mole ratios from one molar ratio to three molar ratio content in the precursor mixture, with the transmittance and average crystallite size increasing from 60% and 26 nm to around 70% and 32.4 nm respectively.

It was represented the impact of post deposition treatment on the structural and optoelectronic properties of NiO_x films.

Substrate temperature ranging from 200 ^oC to 400 ^oC was used in depositing the film, leading to the emergence of 400 ^oC as the optimal temperature as shown by the sharp response observed by the sudden decrease in transmittance at the stated temperature. This strong response to the temperature change indicates a shift in the optical properties of the film. This was also supported by the increased intensity of the diffraction peaks (111) and (200), coupled with the emergence of peak on the (220) plane of the bunsenite structure. The films below 350 ^oC exhibited high transmittance between 85 to 90 % but are amorphous, with a mix of crystalline and amorphous phases observed at 350 ^oC. Which shows the vitality of the fuel idea into the chemical spray pyrolysis in general and especially in ultrasonic spray pyrolysis technique. In current work as a fuel was used acetylacetone in three different mole ratios (1-3).

Increased amount of acetylacetone fuel ratio in the precursor solution led to the possibility of depositing NiO_x at slightly below 400 ^oC and increased crystallite size of the film from 26.0 to 32.4 nm using 1 and 3 molar ratios respectively at 400 ^oC. Annealing the $NiNO_3$:AcAcH 5:3 film at 500 ^oC led to the densification of the film and decrease in film thickness from 114 nm to 57nm.

The deposited films exhibited high resistivity (from 10^4 to 10^6 $\Omega \cdot cm$), which is usual for NiO_x films, with post-deposition treatments not making the resistivity better.

SUMMARY

The growing demand for energy in the world in tandem with the growing population and need to protect the environment raises the question of how to meet it in a sustainable way. This led to the choice of energy materials as one of the possible renewable energies that are of interest due to its abundance, renewability, and massive potential.

In this study we investigated development of nickel oxide thin film by USP deposition method. The films were deposited on borosilicate glass using a nickel nitrate salt and acetylacetone. The impact of deposition temperature was first examined to determine the optimal temperature by varying the substrate temperature from 200 ^{o}C to 400 ^{o}C. On characterization with UV-Vis spectroscopy, X-ray diffractometry, 400 ^{o}C was concluded to be the optimal temperature. The fuel component (acetylacetone) of the precursor mix was varied between 1 to 3 molar ratio to 5 molar ratio of nickel nitrate, and the effect of the molar ratio change was monitored. The films deposited were characterized using X-ray diffraction, scanning electron microscopy, UV-Vis spectroscopy, and van der Pauw measurements. Highest crystallite size and transparency of 32.4 nm and 70% respectively was obtained in films made from the highest acetylacetone component $NiNO_3$:AcAcH 5:3. Band gap of the films decreased from 3.61 to 3.53 eV as the molar ratio of acetylacetone fuel in the precursor mix increased from 5:1 to 5:3.

The implementation of the acetylacetone as fuel idea brought about the possibility of depositing NiO_x thin film at slightly below 400 ^{o}C. This is made possible by the exothermic reaction generating more heat for the combustion process. Post deposition annealing of $NiNO_3$:AcAcH 5:3 film at 500 ^{o}C in air led to densification of the film reducing the thickness halfway from 114 nm to 57 nm.

Post-deposition treatments slightly improved the electrical properties of the NiO_x films. However, for further improvement of the electrical properties (carrier concentration, mobility) of the film to be applicable as a hole transport layer in solar cells various doping strategy should be implemented.

LIST OF REFERENCES

[1] K. O. Ukoba, A. C. Eloka-Eboka, and F. L. Inambao, "Review of nanostructured NiO thin film deposition using the spray pyrolysis technique," *Renewable and Sustainable Energy Reviews*, vol. 82. Elsevier Ltd, pp. 2900–2915, Feb. 01, 2018. doi: 10.1016/j.rser.2017.10.041.

[2] A. Qazi *et al.*, "Towards Sustainable Energy: A Systematic Review of Renewable Energy Sources, Technologies, and Public Opinions," *IEEE Access*, vol. 7, pp. 63837–63851, 2019, doi: 10.1109/ACCESS.2019.2906402.

[3] S. Kim, H. Van Quy, and C. W. Bark, "Photovoltaic technologies for flexible solar cells: beyond silicon," *Materials Today Energy*, vol. 19. Elsevier Ltd, Mar. 01, 2021. doi: 10.1016/j.mtener.2020.100583.

[4] G. M. Wilson *et al.*, "The 2020 photovoltaic technologies roadmap," *Journal of Physics D: Applied Physics*, vol. 53, no. 49. IOP Publishing Ltd, Dec. 02, 2020. doi: 10.1088/1361-6463/ab9c6a.

[5] R. Gross, M. Leach, and A. Bauen, "Progress in renewable energy," 2003. [Online]. Available: www.elsevier.com/locate/envint

[6] L. Filipovic *et al.*, "Methods of simulating thin film deposition using spray pyrolysis techniques," *Microelectron Eng*, vol. 117, pp. 57–66, Apr. 2014, doi: 10.1016/j.mee.2013.12.025.

[7] A. Nakaruk, D. Ragazzon, and C. C. Sorrell, "Anatase thin films by ultrasonic spray pyrolysis," *J Anal Appl Pyrolysis*, vol. 88, no. 1, pp. 98–101, 2010, doi: 10.1016/j.jaap.2010.03.001.

[8] R. Romero, F. Martin, J. R. Ramos-Barrado, and D. Leinen, "Synthesis and characterization of nanostructured nickel oxide thin films prepared with chemical spray pyrolysis," in *Thin Solid Films*, Jun. 2010, pp. 4499–4502. doi: 10.1016/j.tsf.2009.12.016.

[9] K. Sajilal and A. M. Ezhil Raj, "Effect of thickness on structural and magnetic properties of NiO thin films prepared by chemical spray pyrolysis (CSP) technique," *Mater Lett*, vol. 164, pp. 547–550, Feb. 2016, doi: 10.1016/j.matlet.2015.11.065.

[10] S. A. Mahmoud, A. Shereen, and M. A. Tarawnh, "Structural and Optical Dispersion Characterisation of Sprayed Nickel Oxide Thin Films," *Journal of Modern Physics*, vol. 02, no. 10, pp. 1178–1186, 2011, doi: 10.4236/jmp.2011.210147.

[11] C. Fang *et al.*, "All-vacuum deposited perovskite solar cells with glycine modified NiOx hole-transport layers," *RSC Adv*, vol. 12, no. 18, pp. 10863–10869, Apr. 2022, doi: 10.1039/d2ra01360f.

[12] Q. Cui *et al.*, "Charge transfer modification of inverted planar perovskite solar cells by NiOx/Sr:NiOxbilayer hole transport layer," *Chinese Physics B*, vol. 31, no. 3, Feb. 2022, doi: 10.1088/1674-1056/ac1fda.

[13] M. Jlassi, I. Sta, M. Hajji, and H. Ezzaouia, "NiO thin films synthesized by sol-gel: Potentiality for the realization of antireflection layer for silicon based solar cell applications," *Surfaces and Interfaces*, vol. 6, pp. 218–222, Mar. 2017, doi: 10.1016/j.surfin.2016.10.006.

[14] S. Kakherskyi *et al.*, "Structural, microstructural, chemical, and optical properties of NiO nanocrystals and films obtained by 3D printing," *Appl Phys A Mater Sci Process*, vol. 127, no. 9, Sep. 2021, doi: 10.1007/s00339-021-04847-5.

[15] J. D. Desai, "Nickel oxide thin films by spray pyrolysis," *Journal of Materials Science: Materials in Electronics*, vol. 27, no. 12, pp. 12329–12334, Dec. 2016, doi: 10.1007/s10854-016-5617-8.

[16] M. M. Gomaa, M. Boshta, B. S. Farag, and M. B. S. Osman, "Structural and optical properties of nickel oxide thin films prepared by chemical bath deposition and by spray pyrolysis techniques," *Journal of Materials Science: Materials in Electronics*, vol. 27, no. 1, pp. 711–717, Jan. 2016, doi: 10.1007/s10854-015-3807-4.

[17] R. S. Kate, S. C. Bulakhe, and R. J. Deokate, "Effect of Substrate Temperature on Properties of Nickel Oxide (NiO) Thin Films by Spray Pyrolysis," *J Electron Mater*, 2019, doi: 10.1007/s11664-019-07074-0.

[18] V. H. López-Lugo, M. García-Hipólito, A. Rodríguez-Gómez, and J. C. Alonso-Huitrón, "Fabrication of Li-Doped NiO Thin Films by Ultrasonic Spray Pyrolysis and Its Application in Light-Emitting Diodes," *Nanomaterials*, vol. 13, no. 1, Jan. 2023, doi: 10.3390/nano13010197.

[19] L. Cattin, B. A. Reguig, A. Khelil, M. Morsli, K. Benchouk, and J. C. Bernède, "Properties of NiO thin films deposited by chemical spray pyrolysis using different precursor solutions," *Appl Surf Sci*, vol. 254, no. 18, pp. 5814–5821, Jul. 2008, doi: 10.1016/j.apsusc.2008.03.071.

[20] M. N. Chaudhari, "Thin film Deposition Methods: A Critical Review," *Int J Res Appl Sci Eng Technol*, vol. 9, no. VI, pp. 5215–5232, Jun. 2021, doi: 10.22214/ijraset.2021.36154.

[21] K. L. Chopra, P. D. Paulson, and V. Dutta, "Thin-film solar cells: An overview," *Progress in Photovoltaics: Research and Applications*, vol. 12, no. 2–3, pp. 69–92, 2004, doi: 10.1002/pip.541.

[22] A. Mavlonov *et al.*, "A review of Sb2Se3 photovoltaic absorber materials and thin-film solar cells," *Solar Energy*, vol. 201. Elsevier Ltd, pp. 227–246, May 01, 2020. doi: 10.1016/j.solener.2020.03.009.

[23] C. Anrango-Camacho, K. Pavón-Ipiales, B. A. Frontana-Uribe, and A. Palma-Cando, "Recent Advances in Hole-Transporting Layers for Organic Solar Cells," *Nanomaterials*, vol. 12, no. 3. MDPI, Feb. 01, 2022. doi: 10.3390/nano12030443.

[24] M. Napari, T. N. Huq, R. L. Z. Hoye, and J. L. MacManus-Driscoll, "Nickel oxide thin films grown by chemical deposition techniques: Potential and challenges in next-generation rigid and flexible device applications," *InfoMat*, vol. 3, no. 5. Blackwell Publishing Ltd, pp. 536–576, May 01, 2021. doi: 10.1002/inf2.12146.

[25] A. T. Oluwabi *et al.*, "Combinative solution processing and Li doping approach to develop p-type NiO thin films with enchanced electrical properties," *Front Mater*, vol. 10, Feb. 2023, doi: 10.3389/fmats.2023.1060420.

[26] C. C. Diao, C. Y. Huang, C. F. Yang, and C. C. Wu, "Morphological, optical, and electrical properties of p-type nickel oxide thin films by nonvacuum deposition," *Nanomaterials*, vol. 10, no. 4, Apr. 2020, doi: 10.3390/nano10040636.

[27] X. Yin, Y. Guo, H. Xie, W. Que, and L. B. Kong, "Nickel Oxide as Efficient Hole Transport Materials for Perovskite Solar Cells," *Solar RRL*, vol. 3, no. 5. Wiley-VCH Verlag, May 01, 2019. doi: 10.1002/solr.201900001.

[28] X. Yin *et al.*, "A new strategy for efficient light management in inverted perovskite solar cell," *Chemical Engineering Journal*, vol. 439, Jul. 2022, doi: 10.1016/j.cej.2022.135703.

[29] B. A. Reguig, A. Khelil, L. Cattin, M. Morsli, and J. C. Bernède, "Properties of NiO thin films deposited by intermittent spray pyrolysis process," *Appl Surf Sci*, vol. 253, no. 9, pp. 4330–4334, Feb. 2007, doi: 10.1016/j.apsusc.2006.09.046.

[30] R. A. Ismail, S. Ghafori, and G. A. Kadhim, "Preparation and characterization of nanostructured nickel oxide thin films by spray pyrolysis," *Applied Nanoscience (Switzerland)*, vol. 3, no. 6, pp. 509–514, Dec. 2013, doi: 10.1007/s13204-012-0152-2.

[31] K. H. Kim, C. Takahashi, Y. Abe, and M. Kawamura, "Effects of Cu doping on nickel oxide thin film prepared by sol-gel solution process," 2014. doi: 10.1016/j.ijleo.2013.11.074.

[32] M. Obaida, A. M. Fathi, I. Moussa, and H. H. Afify, "Characterization and electrochromic properties of NiO thin films prepared using a green aqueous solution by pulsed spray pyrolysis technique," *J Mater Res*, vol. 37, no. 14, pp. 2282–2292, Jul. 2022, doi: 10.1557/s43578-022-00627-w.

[33] D.; Perednis and L. J. Gauckler, "ETH Library Thin Film Deposition Using Spray Pyrolysis," *J Electroceram*, vol. 14, pp. 103–111, 2005, doi: 10.3929/ethz-b-000033131.

[34] D. Jameel and D. A. Jameel, "Thin Film Deposition Processes Electric characterization and solar cell efficiency of Organic/inorganic semiconductor devices. View project Thin Film Deposition Processes," 2015. [Online]. Available:

http://www.aiscience.org/journal/ijmpahttp://creativecommons.org/licenses/by-nc/4.0/

[35] P. S. Patil and L. D. Kadam, "Preparation and characterization of spray pyrolyzed nickel oxide (NiO) thin films," 2007.

[36] A. T. Oluwabi *et al.*, "Application of ultrasonic sprayed zirconium oxide dielectric in zinc tin oxide-based thin film transistor," *J Mater Chem C Mater*, vol. 8, no. 11, pp. 3730–3739, Mar. 2020, doi: 10.1039/c9tc05127a.

[37] R. S. Kate, H. M. Pathan, R. Kalubarme, B. B. Kale, and R. J. Deokate, "Spray pyrolysis: Approaches for nanostructured metal oxide films in energy storage application," *Journal of Energy Storage*, vol. 54. Elsevier Ltd, Oct. 01, 2022. doi: 10.1016/j.est.2022.105387.

[38] A. B. Workie, H. S. Ningsih, and S. J. Shih, "An comprehensive review on the spray pyrolysis technique: Historical context, operational factors, classifications, and product applications," *Journal of Analytical and Applied Pyrolysis*, vol. 170. Elsevier B.V., Mar. 01, 2023. doi: 10.1016/j.jaap.2023.105915.

[39] S. G. Randive and B. J. Lokhande, "Spray pyrolyzed hydrophilic nickel oxide electrodes with nano-granular morphology for a symmetric supercapacitor device," *J Alloys Compd*, vol. 944, May 2023, doi: 10.1016/j.jallcom.2023.169046.

[40] F. Werner, "Hall measurements on low-mobility thin films," *J Appl Phys*, vol. 122, no. 13, Oct. 2017, doi: 10.1063/1.4990470.

[41] "Scanning Electron Microscopy," *https://www.nanoscience.com/techniques/scanning-electron-microscopy/ (accessed 16 March, 2023).*, 2021.

[42] F. Fu *et al.*, "High-efficiency inverted semi-transparent planar perovskite solar cells in substrate configuration," *Nat Energy*, vol. 2, no. 1, Jan. 2017, doi: 10.1038/nenergy.2016.190.

[43] T. Dittrich *et al.*, "Synthesis Control of Charge Separation at Anatase TiO2Thin Films Studied by Transient Surface Photovoltage Spectroscopy," *ACS Appl Mater Interfaces*, vol. 14, no. 38, pp. 43163–43170, Sep. 2022, doi: 10.1021/acsami.2c09032.

[44] Y. Qin *et al.*, "High-quality NiO thin film by low-temperature spray combustion method for perovskite solar cells," *J Alloys Compd*, vol. 810, Nov. 2019, doi: 10.1016/j.jallcom.2019.151970.